

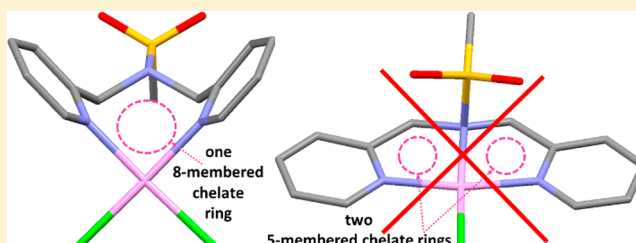
Linear Bidentate Ligands (L) with Two Terminal Pyridyl N-Donor Groups Forming Pt(II)LCl₂ Complexes with Rare Eight-Membered Chelate Rings

Kokila Ranasinghe,¹ Patricia A. Marzilli,¹ Svetlana Pakhomova, and Luigi G. Marzilli*¹

Department of Chemistry, Louisiana State University, Baton Rouge, Louisiana 70803, United States

Supporting Information

ABSTRACT: NMR and X-ray diffraction studies were conducted on Pt(II)LCl₂ complexes prepared with the new N-donor ligands N(SO₂R)Me_ndpa (R = Me, Tol; n = 2, 4). These ligands differ from N(H)dpa (di-2-picolyamine) in having the central N within a tertiary sulfonamide group instead of a secondary amine group and having Me groups at the 6,6'-positions (n = 2) or 3,3',5,5'-positions (n = 4) of the pyridyl rings. The N(SO₂R)3,3',5,5'-Me₄dpa ligands are coordinated in a bidentate fashion in Pt(N(SO₂R)3,3',5,5'-Me₄dpa)Cl₂ complexes, forming a rare eight-membered chelate ring. The sulfonamide N atom did not bind to Pt(II), consistent with indications in the literature that tertiary sulfonamides are unlikely to anchor two meridionally coordinated five-membered chelate rings in solutions of coordinating solvents. The N(SO₂R)6,6'-Me₂dpa ligands coordinate in a monodentate fashion to form the binuclear complexes [trans-Pt(DMSO)Cl₂]₂(N(SO₂R)6,6'-Me₂dpa). The monodentate instead of bidentate N(SO₂R)6,6'-Me₂dpa coordination is attributed to 6,6'-Me steric bulk. These binuclear complexes are indefinitely stable in DMF-d₇, but in DMSO-d₆ the N(SO₂R)6,6'-Me₂dpa ligands dissociate completely. In DMSO-d₆, the bidentate ligands in Pt(N(SO₂R)3,3',5,5'-Me₄dpa)Cl₂ complexes also dissociate, but incompletely; these complexes provide rare examples of association–dissociation equilibria of N,N bidentate ligands in Pt(II) chemistry. Like typical cis-PtLCl₂ complexes, the Pt(N(SO₂R)3,3',5,5'-Me₄dpa)Cl₂ complexes undergo monosolvolysis in DMSO-d₆ to form the [Pt(N(SO₂R)3,3',5,5'-Me₄dpa)(DMSO-d₆)Cl]⁺ cations. However, unlike typical cis-PtLCl₂ complexes, the Pt(N(SO₂R)3,3',5,5'-Me₄dpa)Cl₂ complexes surprisingly do not react readily with the excellent N-donor bioligand guanosine. A comparison of the structural features of over 50 known relevant Pt(II) complexes having smaller chelate rings with those of the very few relevant Pt(II) complexes having eight-membered chelate rings indicates that the pyridyl rings in Pt(N(SO₂R)3,3',5,5'-Me₄dpa)Cl₂ complexes are well positioned to form strong Pt–N bonds. Therefore, the dissociation of the bidentate ligand and the poor biomolecule reactivity of the Pt(N(SO₂R)3,3',5,5'-Me₄dpa)Cl₂ complexes arise from steric consequences imposed by the –CH₂–N(SO₂R)–CH₂– chain in the eight-membered chelate ring.



INTRODUCTION

New properties can be introduced into metal complexes by linking dangling groups with targeting moieties or fluorophores onto carrier ligands. Typically, the most useful linking chemistry avoids creating new asymmetric centers in the complexes, especially when the ultimate goal is to identify a diagnostic or therapeutic agent. Often the central N atom of N,N',N''-donor tridentate ligands (L^{tri}) is used to attach the dangling group (Figure 1).^{1–15} Various metal complexes of tridentate-bound ligand derivatives of di-2-picolyamine (N(H)dpa) or diethylenetriamine (dien) with a suitable group attached to the central N possess useful properties, such as enhanced targeting ability,^{2,7,8} fluorescence,^{3,10,13} high anticancer/antitumor activity,^{9,11,12} or new bioconjugation chemistry.^{4–6} In almost all cases, the dangling group is attached to the chelate ligand via a N–C bond.

To expand the scope of dangling-group and donor-group properties that can be employed, we have been investigating N(SO₂R)dpa-type (Figure 2) and N(SO₂R)dien-type ligands

[R = Me, *p*-tolyl (Tol)], in which the dangling group is attached via a N–S bond. In addition, the central N-donor atom is part of a tertiary sulfonamide group, which normally binds to metals only when part of macrocyclic ligands. Nevertheless, the N(SO₂R)dpa- and N(SO₂R)dien-type ligands function as a new class of tridentate ligands and form *fac*-[Re(CO)₃(N(SO₂R)dpa)]PF₆⁴ and *fac*-[Re(CO)₃(N(SO₂R)dien)]PF₆⁵ complexes that are the first examples of any metal complex with the sulfonamide as part of a noncyclic linear tridentate ligand having a normal metal–N(sulfonamide) bond length (~2.2 Å).^{4,5} The relevance of such Re(I) complexes to the development of ^{99m}Tc(I) and Re(I) diagnostic and therapeutic radiopharmaceutical agents has been discussed.^{4,5} More recently, closely analogous complexes of Mn(I) have been described.^{16,17}

Received: July 12, 2018

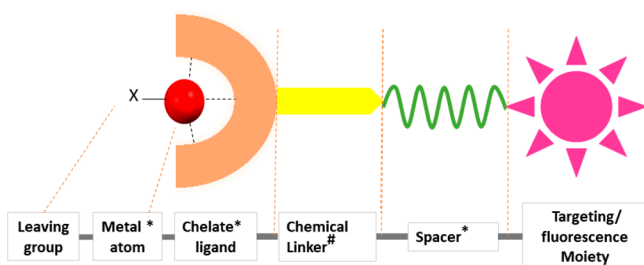


Figure 1. Components of a biological targeting therapeutic or diagnostic metal-containing agent. The label * denotes a component with no geometrical or optical isomers. The label # indicates a nonchiral linking component attached to the central donor of the chelate ligand, thereby avoiding the introduction of geometrical or optical isomers.

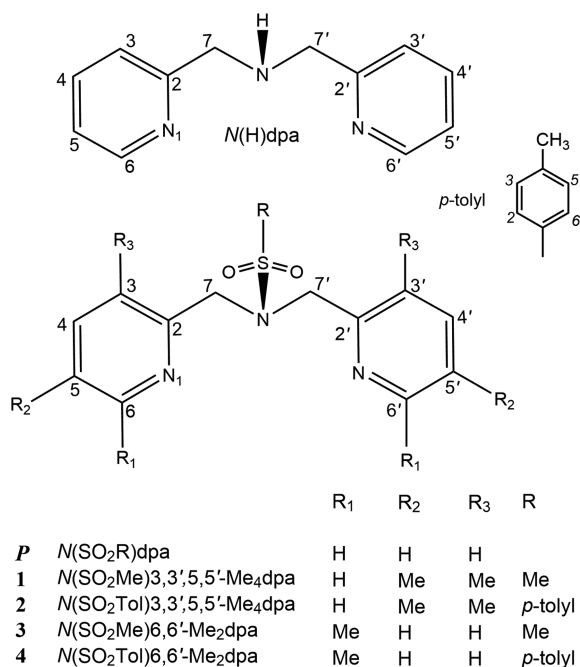


Figure 2. Numbering scheme for *N*(H)dpa and *N*(SO₂R)dpa, the parent (*P*) ligand framework for *N*(SO₂R)Me_{*n*}dpa ligands as follows: *N,N*-bis(3,5-dimethyl-2-picolyl)methanesulfonamide, *N*(SO₂Me)-3,3',5,5'-Me₄dpa (**1**); *N,N*-bis(3,5-dimethyl-2-picolyl)-*p*-tolylsulfonamide, *N*(SO₂Tol)3,3',5,5'-Me₄dpa (**2**); *N,N*-bis(6-methyl-2-picolyl)methanesulfonamide, *N*(SO₂Me)6,6'-Me₂dpa (**3**); and *N,N*-bis(6-methyl-2-picolyl)-*p*-tolylsulfonamide, *N*(SO₂Tol)6,6'-Me₂dpa (**4**). The numbering of the *p*-tolyl group is in *italics* to prevent confusion with the numbering of the pyridyl rings.

Resonance stabilization within the sulfonamide group causes the sulfonamide nitrogen to lack a readily available lone pair of electrons for metal coordination. For a M–N bond to form, the bond must be energetically favorable enough to convert the hybridization of the sulfonamide N from sp² (resonance-stabilized) to sp³ (stabilized by the M–N bond). A key factor favoring coordination of the tertiary sulfonamide N of *N*(SO₂R)dpa- and *N*(SO₂R)dien-type ligands to Re(I) is the formation of two adjacent five-membered chelate rings, the most favorable ring size for chelate formation. In this study, we investigated whether under typical synthetic conditions a Pt–N(sulfonamide) bond could also form in Pt(II) complexes of *N*(SO₂R)dpa-type ligands; in such a case, new types of dangling groups could be employed with Pt(II) complexes that

possess a metal center, forming agents known to have widespread use in biomedicine. In particular, Pt(II) complexes with chelating ligands having dangling groups^{9–15,18,19} have been widely explored because such complexes often exhibit anticancer or antiviral activity.^{9,11,12,19}

Adduct formation with biological molecules is usually not a key feature for biological applications of Re(I) complexes. However, Pt(II) complexes typically act by forming adducts and require one or two leaving groups for functionality. Because aromatic ¹H NMR signals complicate studies of adduct formation, we have utilized four new *N*(SO₂R)Me_{*n*}dpa ligands differing in methyl substitution patterns on the pyridyl rings (Figure 2) to prepare Pt(II) complexes.

Previous studies have shown that *N*(H)dpa (Figure 2) and related ligands readily form [Pt(L^{III})Cl]⁺ complexes.^{20,21} However, the new *N*(SO₂R)Me_{*n*}dpa ligands form Pt(II) complexes with bidentate *N*(SO₂R)Me_{*n*}dpa ligands having an eight-membered chelate ring, in which the tertiary sulfonamide nitrogen is not bound to Pt(II) but serves as an atom in the –CH₂–N(SO₂R)–CH₂– chain of the chelate ring. Structural characterizations of Pt(II) complexes with bidentate ligands having eight-membered chelate rings such as those found here are very few in number compared with bifunctional Pt(II) complexes with smaller five-, six-, or seven-membered chelate rings of bidentate pyridyl/imidazolyl ligands^{22–44} or with two pyridyl/imidazolyl monodentate ligands.^{45–49} The rarity and unusual properties of the new bifunctional Pt(II) compounds with a large eight-membered chelate ring described herein led us to compare their structural features with those of related bifunctional Pt(II) complexes. The relevance of binding at G residues in DNA by anticancer-active Pt(II) compounds^{22,27,37,38,49} has led to many studies of adduct formation of guanine derivatives (G). Mono- and bifunctional Pt(II) chloro complexes bearing carrier ligands with five- and six-membered chelate rings readily form G adducts in various solvents.^{20,21,50} Upon adduct formation, guanine ligands can even disrupt and open a chelate ring.⁵¹ Surprisingly, the new Pt(II) compounds do not readily form G adducts.

EXPERIMENTAL SECTION

Starting Materials. Methanesulfonamide (MeSO₂NH₂), *p*-tolylsulfonamide (TolSO₂NH₂), 2,3,5-collidine, 6-methyl-2-pyridine-methanol, tetraethylammonium chloride ([Et₄N]Cl), and K₂PtCl₄ were used as received from Aldrich. *cis*-Pt(DMSO)₂Cl₂,⁵² 2-(chloromethyl)-6-methylpyridine,⁵³ and 2-(chloromethyl)-3,5-dimethylpyridine⁵⁴ were prepared by known methods.

NMR Measurements. ¹H NMR spectra were recorded on a 400 MHz or an Avance III Prodigy 500 MHz Bruker spectrometer. Peak positions are relative to tetramethylsilane (TMS) or the residual solvent peak with TMS as the reference. All of the NMR data were processed with TopSpin and MestReNova software. A presaturation pulse to suppress the water peak was employed when necessary.

Mass Spectrometric Measurements. High-resolution mass spectra were recorded on an Agilent 6210 electrospray ionization (ESI) time of flight (TOF) LC–MS mass spectrometer.

X-ray Data Collection and Structure Determination. Diffraction data were collected on a Bruker Kappa Apex II DUO CCD diffractometer with Mo Kα radiation (λ = 0.71073 Å), equipped with an Oxford Cryosystems Cryostream. All of the X-ray structures were determined by direct methods and difference Fourier techniques and refined by full-matrix least-squares using SHELXL2014⁵⁵ with H atoms in idealized positions.

General Synthesis of Ligands. A solution of the desired 2-(chloromethyl)pyridine derivative (~6 mmol), K₂CO₃ (~1.7 g, 12 mmol), and the appropriate sulfonamide (~2.5 mmol) in acetonitrile

(95 mL) was heated at reflux under nitrogen for 18 h. After removal of acetonitrile under reduced pressure, the residue was dissolved in water (45 mL), and the solution was extracted with CH_2Cl_2 (3×45 mL). The organic layers were combined, washed with saturated aqueous sodium chloride solution, dried over sodium sulfate, and taken to dryness under reduced pressure. The residue was dissolved in 80:20 ethyl acetate/hexane and purified by chromatography on a silica column with the same eluent. Fractions were collected and spotted on TLC plates using the same eluent. The cleanest fractions, as assessed by ^1H NMR spectroscopy, were combined and taken to dryness by rotary evaporation to afford the desired ligand in sufficient purity to use in the synthesis of the corresponding Pt(II) complex.

N(SO₂Me)3,3',5,5'-Me₄dpa (1). The general ligand synthesis described above was carried out with 2-(chloromethyl)-3,5-dimethylpyridine (0.98 g, 6.2 mmol) and MeSO_2NH_2 (0.23 g, 2.4 mmol) and produced an orange residue that was purified by column chromatography to afford *N(SO₂Me)3,3',5,5'-Me₄dpa* as a white solid (0.54 g, 67% yield). ^1H NMR signals (ppm) in CDCl_3 : 8.19 (s, 2H, H6/6'), 7.23 (s, 1H, H4/4'), 4.60 (s, 4H, CH_2), 3.15 (s, 3H, CH_3), 2.28 (s, 6H, CH_3), 2.21 (s, 6H, CH_3). ^1H NMR signals (ppm) in $\text{DMSO}-d_6$: 8.17 (s, 2H, H6/6'), 7.33 (s, 2H, H4/4'), 4.45 (s, 4H, CH_2), 3.13 (s, 3H, CH_3), 2.23 (s, 6H, CH_3), 2.12 (s, 6H, CH_3). ESI-MS (m/z): $[\text{M} + \text{H}]^+ = 334.1596$ (calcd 334.1584).

N(SO₂Tol)3,3',5,5'-Me₄dpa (2). The general ligand synthesis with 2-(chloromethyl)-3,5-dimethylpyridine (1.04 g, 6.6 mmol) and ToSO_2NH_2 (0.46 g, 2.6 mmol) yielded an orange residue that was purified by column chromatography to afford *N(SO₂Tol)3,3',5,5'-Me₄dpa* as a pale-yellow solid (0.88 g, 79% yield). ^1H NMR signals (ppm) in CDCl_3 : 7.98 (s, 2H, H6/6'), 7.70 (d, $J = 8.1$ Hz, 2H, H2/6), 7.26 (masked by the solvent peak, 2H, H3/5), 7.07 (s, 2H, H4/4'), 4.48 (s, 4H, CH_2), 2.43 (s, 3H, CH_3), 2.25 (s, 6H, CH_3), 2.19 (s, 6H, CH_3). ^1H NMR signals (ppm) in $\text{DMSO}-d_6$: 7.94 (s, 2H, H6/6'), 7.62 (d, $J = 7.8$ Hz, 2H, H2/6), 7.32 (d, $J = 7.9$ Hz, 2H, H3/5), 7.21 (s, 2H, H4/4'), 4.41 (s, 4H, CH_2), 2.39 (s, 3H, CH_3), 2.16 (s, 6H, CH_3), 2.13 (s, 6H, CH_3). ESI-MS (m/z): $[\text{M} + \text{H}]^+ = 410.1876$ (calcd 410.1897).

N(SO₂Me)6,6'-Me₂dpa (3). The general ligand synthesis with 2-(chloromethyl)-6-methylpyridine (0.90 g, 6.4 mmol) and MeSO_2NH_2 (0.24 g, 2.5 mmol) yielded an orange residue that was purified by column chromatography to afford *N(SO₂Me)6,6'-Me₂dpa* as a colorless oil (0.68 g, 88% yield). ^1H NMR signals (ppm) in CDCl_3 : 7.55 (t, $J = 7.7$ Hz, 2H, H4/4'), 7.18 (d, $J = 7.7$ Hz, 2H, H5/5'), 7.05 (d, $J = 7.7$ Hz, 2H, H3/3'), 4.54 (s, 4H, CH_2), 3.15 (s, 3H, CH_3), 2.51 (s, 6H, CH_3). ^1H NMR signals (ppm) in $\text{DMSO}-d_6$: 7.63 (t, $J = 7.7$ Hz, 2H, H4/4'), 7.12 (d, $J = 7.8$ Hz, 4H, H3/3' and H5/5'), 4.42 (s, 4H, CH_2), 3.14 (s, 3H, CH_3), 2.41 (s, 6H, CH_3). ESI-MS (m/z): $[\text{M} + \text{H}]^+ = 306.1269$ (calcd 306.1271).

N(SO₂Tol)6,6'-Me₂dpa (4). The general ligand synthesis with 2-(chloromethyl)-6-methylpyridine (1.00 g, 7.1 mmol) and ToSO_2NH_2 (0.58 g, 3.4 mmol) yielded an orange residue that was purified by column chromatography to afford *N(SO₂Tol)6,6'-Me₂dpa* as a yellow oil (1.14 g, 89% yield). ^1H NMR signals (ppm) in CDCl_3 : 7.71 (d, $J = 8.1$ Hz, 2H, H2/6), 7.43 (t, $J = 7.7$ Hz, 2H, H4/4'), 7.24 (d, $J = 8.1$ Hz, 2H, H3/5), 7.14 (d, $J = 7.8$ Hz, 2H, H3/3'), 6.92 (d, $J = 7.7$ Hz, 2H, H5/5'), 4.56 (s, 4H, CH_2), 2.42 (s, 3H, CH_3), 2.37 (s, 6H, CH_3). ^1H NMR signals (ppm) in $\text{DMSO}-d_6$: 7.67 (d, $J = 8.2$ Hz, 2H, H2/6), 7.53 (t, $J = 7.7$ Hz, 2H, H4/4'), 7.33 (d, $J = 8.0$ Hz, 2H, H3/5), 7.04 (quasi-t, 4H, H3/3' and H5/5'), 4.43 (s, 4H, CH_2), 2.37 (s, 3H, CH_3), 2.28 (s, 6H, CH_3). ESI-MS (m/z): $[\text{M} + \text{H}]^+ = 382.1591$ (calcd 382.1584).

General Synthesis of Complexes. A stirred solution of the ligand (0.1 mmol) and *cis*-Pt(DMSO)₂Cl₂ (0.1 mmol) in methanol (5 mL) was heated at reflux overnight (~16 h). The yellow precipitate that formed overnight was collected by filtration, washed with methanol and ether, and air-dried (method A). X-ray-quality crystals were obtained by mixing equal volumes (1 mL) of solutions of *cis*-Pt(DMSO)₂Cl₂ (12.5 mM) and the ligand (12.5 mM) in acetonitrile and allowing the mixture to stand at room temperature. Needlelike crystals were obtained within 2 days to 2 weeks (method B). The ^1H

NMR data were identical for the products obtained by methods A and B.

Pt(N(SO₂Me)3,3',5,5'-Me₄dpa)Cl₂ (5). With *N(SO₂Me)3,3',5,5'-Me₄dpa* (1) (33 mg, 0.1 mmol) and *cis*-Pt(DMSO)₂Cl₂ (42 mg, 0.1 mmol), method A afforded a pale-yellow solid (26 mg, 44% yield). Yellow crystals obtained by method B were characterized by single-crystal X-ray crystallography. ^1H NMR signals (ppm) in $\text{DMSO}-d_6$: 8.98 (s, 2H, H6/6'), 7.56 (s, 2H, H4/4'), 5.99 (d, $J = 14.7$ Hz, 2H, CH_2), 5.37 (d, $J = 14.9$ Hz, 2H, CH_2), 3.35 (s, 3H, CH_3), 2.37 (s, 6H, CH_3), 2.23 (s, 6H, CH_3). ESI-MS (m/z): $[\text{M} - \text{H}]^- = 597.0450$ (calcd 597.0463).

Pt(N(SO₂Tol)3,3',5,5'-Me₄dpa)Cl₂ (6). With *N(SO₂Tol)3,3',5,5'-Me₄dpa* (2) (41 mg, 0.1 mmol) and *cis*-Pt(DMSO)₂Cl₂ (42 mg, 0.1 mmol), method A afforded a pale-yellow solid (25 mg, 37% yield). Yellow crystals obtained by method B were characterized by single-crystal X-ray crystallography. ^1H NMR signals (ppm) in $\text{DMSO}-d_6$: 8.90 (s, 2H, H6/6'), 8.03 (d, $J = 8.2$ Hz, 2H, H2/6), 7.60 (d, $J = 8.1$ Hz, 2H, H3/5), 7.56 (s, 2H, H4/4'), 5.55 (d, $J = 14.3$ Hz, 2H, CH_2), 5.47 (d, $J = 14.3$ Hz, 2H, CH_2), 2.45 (s, 6H, CH_3), 2.21 (s, 6H, CH_3); the phenyl methyl signal was masked by the solvent peak. ESI-MS (m/z): $[\text{M} + \text{H}]^+ = 676.0926$ (calcd 676.0913).

[trans-Pt(DMSO)Cl₂]₂(N(SO₂Me)6,6'-Me₂dpa) (7). With *N(SO₂Me)6,6'-Me₂dpa* (3) (30 mg, 0.1 mmol) and *cis*-Pt(DMSO)₂Cl₂ (42 mg, 0.1 mmol), method A afforded a pale-yellow solid (16 mg, 28% yield). ^1H NMR signals (ppm) in $\text{DMSO}-d_6$: 7.85 (t, $J = 7.8$ Hz, 2H, H4/4'), 7.68 (d, $J = 7.9$ Hz, 2H, H3/3'), 7.46 (d, $J = 7.8$ Hz, 2H, H5/5'), 5.55 (s, 4H, CH_2), 3.33 (s, 3H, CH_3), 3.12 (s, 6H, CH_3). ESI-MS (m/z): $[\text{M} + \text{H}]^+ = 993.9522$ (calcd 993.9569).

[trans-Pt(DMSO)Cl₂]₂(N(SO₂Tol)6,6'-Me₂dpa) (8). With *N(SO₂Tol)6,6'-Me₂dpa* (4) (38 mg, 0.1 mmol) and *cis*-Pt(DMSO)₂Cl₂ (42 mg, 0.1 mmol), method A afforded a pale-yellow solid (14 mg, 22% yield). Yellow needle-shaped crystals obtained by method B were characterized by single-crystal X-ray crystallography. ^1H NMR signals (ppm) in $\text{DMSO}-d_6$: 7.91 (d, $J = 8.0$ Hz, 2H, H2/6), 7.76 (t, $J = 7.9$ Hz, 2H, H4/4'), 7.57 (d, $J = 8.0$ Hz, 2H, H3/3'), 7.52 (d, $J = 8.0$ Hz, 2H, H3/5), 7.43 (d, $J = 7.9$ Hz, 2H, H5/5'), 5.46 (s, 4H, CH_2), 3.11 (s, 6H, CH_3), 2.43 (s, 3H, CH_3). ESI-MS (m/z): $[\text{M} + \text{H}]^+ = 1069.9921$ (calcd 1069.9884). The solvent of the clear, pale-yellow filtrate from method A was removed under reduced pressure, leaving a residue. The ^1H NMR spectrum of this residue in $\text{DMSO}-d_6$ showed peaks for free ligand 4 and for ligand 4 bound to Pt(II) in an unsymmetric monodentate fashion.

Isolation of Crystals of *trans*-[Pt(DMSO)Cl₂]₂(N(SO₂Tol)6,6'-Me₂dpa) (8a). In a preparation that led to the isolation of the new complex detected in the residue just mentioned, an aqueous solution of K_2PtCl_4 (0.208 g, 0.5 mmol in 10 mL) was heated to 70 °C and treated with 70 μL (1 mmol) of DMSO followed after 10 min by 4 (191 mg, 0.5 mmol). The mixture was heated and stirred for 1 h at 95 °C. The yellow solid (78 mg, 15% yield) that precipitated was collected by filtration, washed with methanol and ether, and identified as complex 8 by its ^1H NMR spectrum. Overnight this clear yellow filtrate deposited yellow X-ray-quality crystals of 8a (53 mg, 15% yield). The ^1H NMR signals of the crystals of 8a in $\text{DMSO}-d_6$ were identical to those for the complex in the residue obtained with method A (see above). ^1H NMR signals (ppm) in $\text{DMSO}-d_6$: 7.88 (t, $J = 8.0$ Hz, 1H, H4_b), 7.78 (d, $J = 8.0$ Hz, 2H, H2/6), 7.54 (t, $J = 7.9$ Hz, 1H, H4_a), 7.49 (d, $J = 8.0$ Hz, 1H, H3_b), 7.42 (d, $J = 8.0$ Hz, 3H, H3/5 and H5_b), 7.14 (d, $J = 7.9$ Hz, 1H, H3_a), 7.04 (d, $J = 7.9$ Hz, 1H, H5_a), 5.40 (s, 2H, CH_{2b}), 4.50 (s, 2H, CH_{2a}), 3.09 (s, 3H, CH_{3b}), 2.42 (s, 3H, CH_3), 2.27 (s, 3H, CH_{3a}). MALDI-TOF (m/z): $[\text{M} + \text{Na}]^+ = 748.096$ (calcd 748.052).

Solution Studies of 5. A solution of 5 (10 mM) in $\text{DMSO}-d_6$ (solution 1) was monitored by ^1H NMR spectroscopy for at least 21 days. Another 10 mM solution of 5 in $\text{DMSO}-d_6$ was treated with 10 molar equiv of $[\text{Et}_4\text{N}]\text{Cl}$ (10 mg) after 1 day (solution 2). In another experiment, 5 (3.6 mg) was added to a solution of $[\text{Et}_4\text{N}]\text{Cl}$ (100 mM) in $\text{DMSO}-d_6$ to make the solution 10 mM in 5 (solution 3). In a similar experiment, a sufficient amount of ligand 1 (1.3 mg) was added to a solution containing *cis*-Pt(DMSO)₂Cl₂ (10 mM) and $[\text{Et}_4\text{N}]\text{Cl}$ (100 mM) in $\text{DMSO}-d_6$ to make the solution 10 mM in

ligand **1** (solution 4). Another 10 mM solution of **1** in DMSO- d_6 was treated with 1 molar equiv of *cis*-Pt(DMSO) $_2$ Cl $_2$ (1.7 mg) (solution 5). Solutions 2, 3, 4, and 5 were monitored over time by 1 H NMR spectroscopy. Solutions (10 mM) of **6** in DMSO- d_6 or DMF- d_7 (partially dissolved) and **7** and **8** in DMSO- d_6 were kept at 25 °C and monitored by 1 H NMR spectroscopy.

RESULTS AND DISCUSSION

Synthesis of $N(\text{SO}_2\text{R})\text{Me}_n\text{dpa}$ Derivatives and Their Pt(II) Complexes. Our previous synthesis of $N(\text{SO}_2\text{R})\text{dpa}$ ligands⁴ (route 1, Figure 3) utilized commercially available

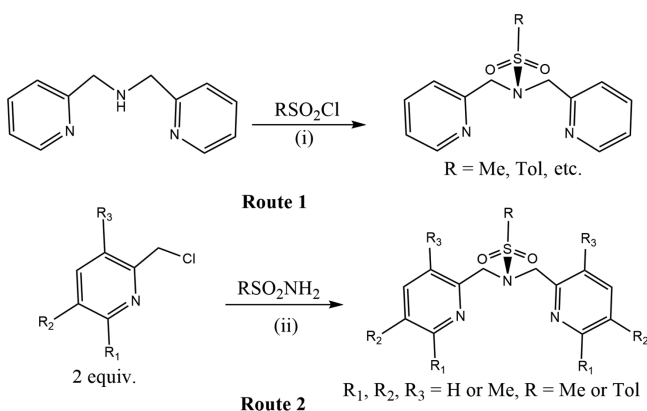


Figure 3. Synthetic routes for the ligands $N(\text{SO}_2\text{R})\text{dpa}$ (route 1) and $N(\text{SO}_2\text{R})\text{Me}_n\text{dpa}$ (route 2). Conditions: (i) dioxane, room temperature, 24 h; (ii) K_2CO_3 , acetonitrile at reflux, N_2 , 18 h.

$N(\text{H})\text{dpa}$ (Figure 2). However, the $N(\text{H})\text{Me}_n\text{dpa}$ parent ligands needed in this study, $N(\text{H})3,3',5,5'\text{-Me}_4\text{dpa}$ and $N(\text{H})6,6'\text{-Me}_2\text{dpa}$, are not commercially available. Thus, the new $N(\text{SO}_2\text{R})\text{Me}_n\text{dpa}$ ligands **1–4** were synthesized by a different route in which the desired 2-chloromethylpyridyl derivative (2 equiv) was coupled with the appropriate sulfonamide under basic conditions (route 2, Figure 3). Ligands **1–4** were treated with *cis*-Pt(DMSO) $_2$ Cl $_2$ in methanol at reflux to obtain complexes **5–8** (Figure 4).

X-ray Structural Results. Crystal data and structural refinement details for **5**, **6**, **8**, and **8a** are summarized in the Supporting Information. ORTEP plots of the molecular structures of the complexes (Figures 5 and 6) show the

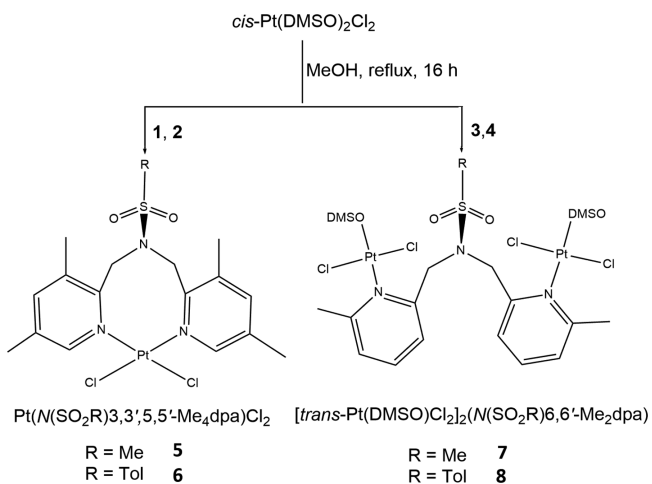


Figure 4. General reaction conditions for the formation of complexes **5–8**.

numbering systems used to describe the solid-state data. Selected bond lengths and angles are reported in Table 1. Crystals of **6** contain two independent molecules in the asymmetric unit, only one of which (**B**) is shown in Figure 6 and used in the discussion. The structural metrics of the two halves of complex **8** are slightly different in the solid state and are reported separately in Table 1 as Pt1 and Pt2.

The molecular structures of the Pt(II) complexes of ligands **1**, **2**, and **4** reveal that the sulfonamide N does not form a Pt–N bond in any of the complexes (**5**, **6**, **8**, and **8a**; Figures 5 and 6). The sulfonamide N of $N(\text{SO}_2\text{Me})6,6'\text{-Me}_2\text{dpa}$ (**3**) also does not bind to Pt(II) (discussed later). The only Pt–N bonds found in this work involve a pyridyl group. All of the Pt–N bonds have lengths (Table 1) falling in the range typically reported for Pt–N(sp^2) bonds (1.99–2.08 Å).^{21,56} The bidentate coordination mode in the Pt($N(\text{SO}_2\text{R})3,3',5,5'\text{-Me}_4\text{dpa}$)Cl $_2$ complexes [R = Me (**5**), R = Tol (**6**); Figure 5] creates a relatively large and uncommon eight-membered chelate ring.

Structural Features Favoring Coordination of Tertiary Sulfonamides. When a tertiary sulfonamide N is bound to a metal center [e.g., Mn(I), Cu(II), Ni(II), Co(II), Re(I)],^{1,4,5,16,17,57,58} the angles around the sulfonamide N atom are consistent with sp^3 hybridization. In contrast, the angles around the tertiary sulfonamide N in **5** and **6** (Table 1) are closer to 120° than to 109.5° (tetrahedral geometry), indicating that sp^2 hybridization of the sulfonamide N atom is retained.

The N–S bond distances are generally longer (1.73–1.78 Å)^{1,4,5,16,17,57,58} in metal complexes with an N-coordinated tertiary sulfonamide than in complexes with an uncoordinated sulfonamide N (1.62–1.64 Å).^{1,4,57,59} Accordingly, the N–S bond distances in the Pt(II) complexes reported here (Table 1) are shorter than those for such known complexes. Shorter N–S bond distances in an uncoordinated sulfonamide group indicate a considerable amount of double-bond character of the N–S bond.^{1,4,60}

Except for *fac*-[Re(CO) $_3$ ($N(\text{SO}_2\text{R})\text{dien}$)]PF $_6$ ⁵ complexes, the $N(\text{SO}_2\text{R})\text{dpa}$ -type ligands are the only linear ligands found thus far to have a bound tertiary sulfonamide in structurally characterized complexes, e.g., *fac*-[Re(CO) $_3$ ($N(\text{SO}_2\text{R})\text{-Me}_n\text{dpa}$)]PF $_6$ (unpublished work using ligands **1–4** reported here), *fac*-[Re(CO) $_3$ ($N(\text{SO}_2\text{R})\text{dpa}$)](PF $_6$ or BF $_4$), and *fac*-[Mn(CO) $_3$ ($N(\text{SO}_2\text{R})\text{dpa}$)]CF $_3$ SO $_3$.^{4,16,17} In these pseudo-octahedral Re(I)/Mn(I) complexes, the three N-donor atoms are facially coordinated. In structurally characterized complexes with other metal centers, the metal-bound tertiary sulfonamide nitrogen is within a macrocyclic ligand. In these structures, the central sulfonamide nitrogen and the two adjacent N-donor atoms occupy the face of an octahedron or have a similar arrangement in complexes with other geometries (such as distorted trigonal-bipyramidal or square-pyramidal).^{4,16,61}

In square-planar Pt(II) complexes, the central donor atom of a tridentate ligand forming two five-membered chelate rings must be able to accommodate the meridional coordination mode. A clear case in which a tertiary sulfonamide group anchors two chelate rings having a meridional disposition has been reported for a square-planar Cu(II) complex of a derivative of cyclam (a cyclic tetradentate macrocyclic N-donor ligand with alternating five- and six-membered chelate rings).⁶¹ One of the four donor nitrogens in the cyclam derivative bears a tosyl group. The angles and other parameters

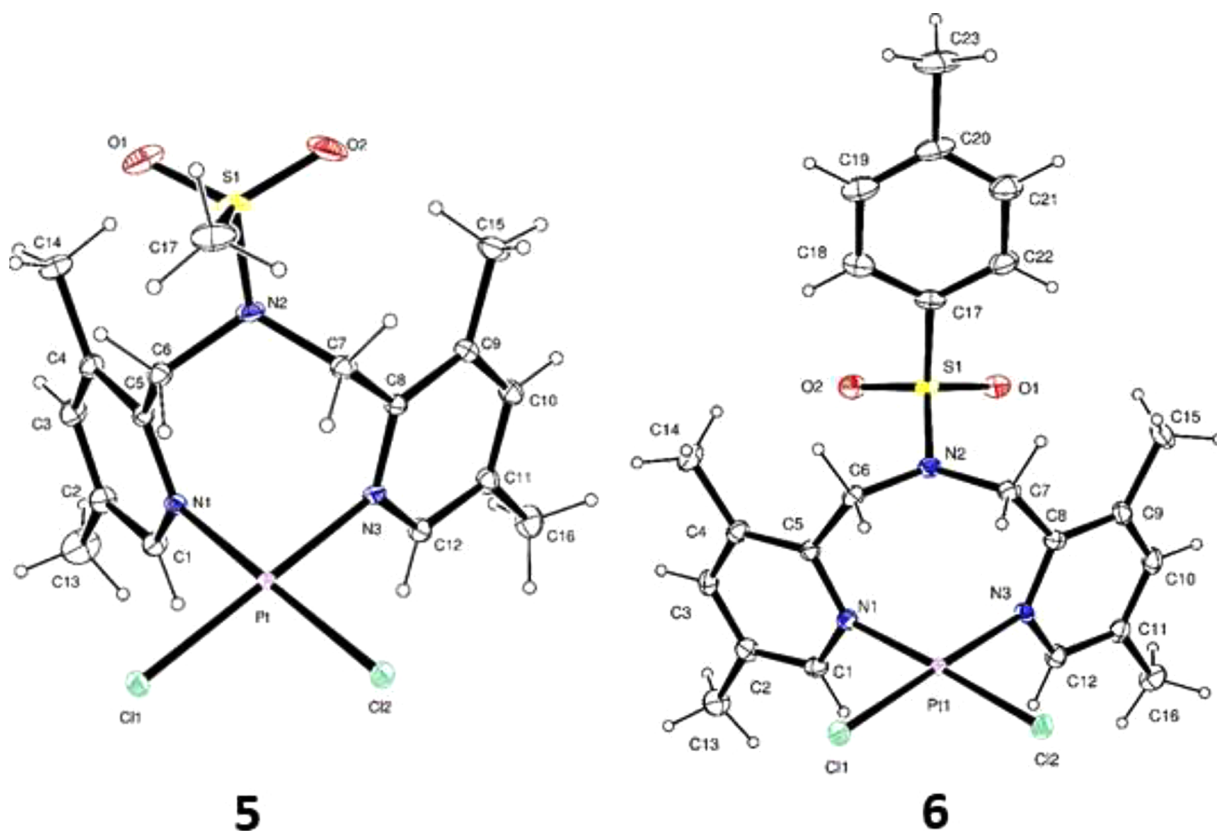


Figure 5. ORTEP plots of the complexes $\text{Pt}(\text{N}(\text{SO}_2\text{Me})_{3,3',5,5'}\text{-Me}_4\text{dpa})\text{Cl}_2$ (**5**) and $\text{Pt}(\text{N}(\text{SO}_2\text{Tol})_{3,3',5,5'}\text{-Me}_4\text{dpa})\text{Cl}_2$ (**6**). Thermal ellipsoids are drawn with 50% probability.

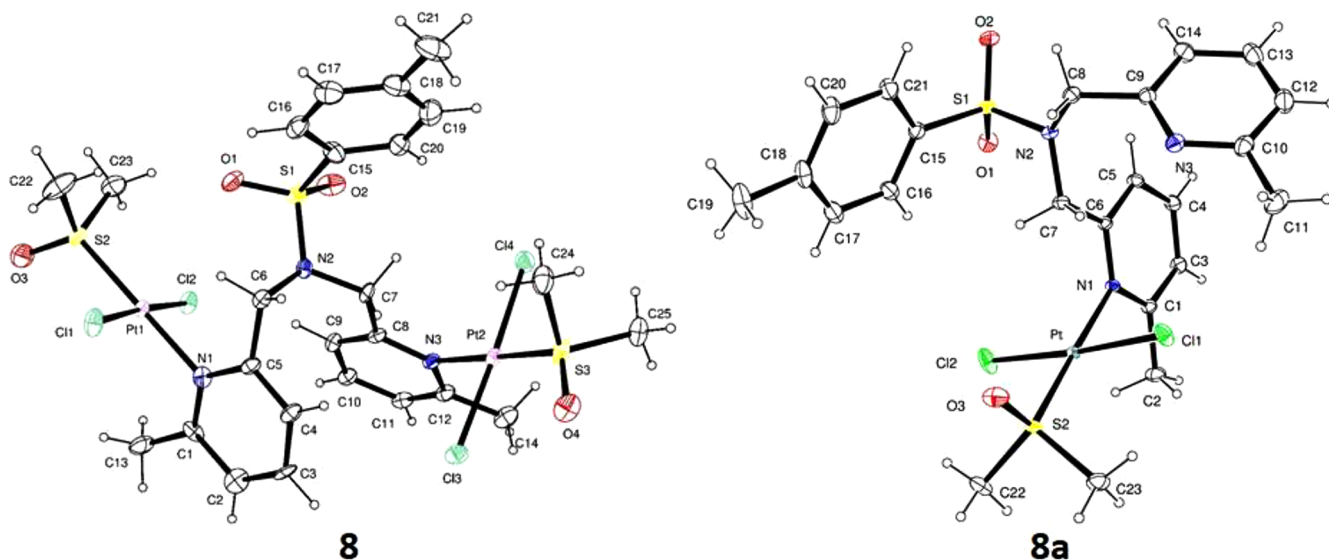


Figure 6. ORTEP plots of the complexes $[\text{trans-Pt}(\text{DMSO})\text{Cl}_2]_2(\text{N}(\text{SO}_2\text{Tol})_{6,6'}\text{-Me}_2\text{dpa})$ (**8**) and $[\text{trans-Pt}(\text{DMSO})\text{Cl}_2](\text{N}(\text{SO}_2\text{Tol})_{6,6'}\text{-Me}_2\text{dpa})$ (**8a**). Thermal ellipsoids are drawn with 50% probability.

involving the sulfonamide N within the sulfonamide group are normal for a coordinated sulfonamide, but the Cu–N(sulfonamide) bond is longer than all of the other Cu–N bonds in the report. In the distorted sulfonamide complex, the Cu(II) atom deviates by ~ 0.2 Å from the planes defined either by all four ligating N atoms or by any three ligating N atoms. However, in the parent cyclam complex, the Cu(II) atom lies in all such planes (deviation of ~ 0.002 Å).

The structural features of complexes with M–N(sulfonamide) bonds reported in the literature, including the Cu cyclam complexes just discussed, suggest a reason why potentially tridentate ligands **1** and **2** coordinate in a bidentate fashion in Pt(II) complexes **5** and **6**, respectively, even when the complexes are prepared using synthetic approaches known to be successful with related ligands having a central amine N-donor.^{20,50,51} These observations lead us to propose that a

Table 1. Selected Bond Distances (Å) and Angles (deg) for Pt(N(SO₂Me)₃,3',5,5'-Me₄dpa)Cl₂ (**5**), Pt(N(SO₂Tol)₃,3',5,5'-Me₄dpa)Cl₂ (**6**), [trans-Pt(DMSO)Cl₂]₂(N(SO₂Tol)₆,6'-Me₂dpa) (**8**), and [trans-Pt(DMSO)Cl₂](N(SO₂Tol)₆,6'-Me₂dpa) (**8a**)

	5	6 (B)	8		8a
			Pt1	Pt2	
Pt–N1	2.023(2)	2.027(3)	2.062(9)	–	2.0757(9)
Pt–N2 ^a	3.693(2)	3.317(3)	3.744(8)	4.51(1)	4.5556(9)
Pt–N3	2.031(2)	2.032(3)	–	2.066(8)	–
Pt–Cl1/3	2.2939(6)	2.2888(8)	2.303(2)	2.297(2)	2.2922(3)
Pt–Cl2/4	2.2990(6)	2.3009(8)	2.304(2)	2.320(3)	2.3030(3)
S1–O1	1.436(3)	1.430(3)	1.429(8)	–	1.4358(10)
S1–O2	1.435(3)	1.434(3)	1.431(7)	–	1.4327(9)
N2–S1	1.6565(19)	1.630(3)	1.642(8)	–	1.6390(10)
Pt–S2/3	–	–	2.217(3)	2.219(3)	2.2218(3)
N1–Pt–N3	87.98(8)	95.21(10)	–	–	–
S1–N2–C6	113.77(17)	118.10(2)	116.0(6)	–	116.85(8)
S1–N2–C7	113.83(17)	117.0(2)	118.9(6)	–	118.66(7)
C6–N2–C7	114.78(17)	121.30(2)	115.3(7)	–	116.15(9)
N1–Pt–Cl2/4	176.99(6)	176.62(8)	89.4(2)	–	89.70(3)
N1–Pt–Cl1/3	89.51(6)	86.18(8)	86.9(2)	–	87.15(3)
N3–Pt–Cl1/3	175.88(6)	178.51(7)	–	86.2(2)	–
N3–Pt–Cl2/4	90.22(6)	86.92(8)	–	89.4(2)	–
Cl1/3–Pt–Cl2/4	92.15(2)	90.66(3)	176.05(9)	175.57(9)	175.68(12)
dihedral angle ^b	77.18, 82.61	86.47, 87.17	75.13	82.91	85.23
Pt–N–centroid	174.82, 174.23	169.84, 166.56	173.49	179.52	174.16
N1–N3 ^a	2.816(3)	2.998(4)	5.15(1)	–	4.632(1)

^aNonbonded distance between the two atoms. ^bAngle between the coordination plane (defined by the Pt, N1, N3, and two Cl atoms) and the pyridyl ring planes.

nitrogen atom in a central tertiary sulfonamide group with two adjacent five-membered chelate rings can act as a donor in a tridentate ligand only when the ligand is facially coordinated.

Comparison of Structural Features of the New Pt(N(SO₂R)₃,3',5,5'-Me₄dpa)Cl₂ Complexes with Those of Other Bifunctional Pt(II) Complexes. The eight-membered chelate ring in the Pt(N(SO₂R)Me_ndpa)Cl₂ complexes is a rare and hence interesting feature. Indeed, only a few types of Pt(II) complexes containing eight-membered chelate rings have molecular structures reported to the Cambridge Crystallographic Data Centre (CCDC). Most examples have very closely related bidentate ligand derivatives with Pt(II) bound to the pyridyl N of a fused bicyclic 7-azaindol-1-yl group.^{39,40,43} Only one Pt(II) complex contains a linear ligand terminated with two simple aromatic rings (pyridyl). Other complexes commonly have macrocyclic N-donor (mostly sp³) ligands bound in a bidentate mode.^{41,42} In the CCDC database we found only three Pt(II) complexes with an eight-membered chelate ring that contain two aromatic-ring nitrogens (pyridyl/imidazolyl) and two halides as the other ligating atoms;^{42–44} however, at the time of our analysis there were 7, 17, and 108 complexes having seven-, six-, and five-membered chelate rings, respectively.^{22–38} Structural data for 53 complexes (all of the complexes containing eight-, seven-, and six-membered chelate rings plus 26 randomly chosen complexes of five-membered chelate rings) were utilized in the following comparison with the structural data for **5** and **6**.

In bifunctional Pt(II) complexes with two cis aromatic planar N-donor rings (one bidentate or two monodentate), the tilting of each ring can be gauged by the dihedral angle between the plane of the aromatic ring (defined by the C and

N atoms in the ring) and the coordination plane (defined by Pt and the four ligating atoms). If the dihedral angle is close to 90°, the aromatic ring is described as not being tilted. As the angle decreases, the ring is said to become more tilted. The two pyridyl rings in **5** and **6** are only slightly tilted, with dihedral angles ranging from 77° to 87° (Table 1); thus, the eight-membered ring allows the pyridyl rings to be oriented roughly perpendicular to the coordination plane. In contrast, other known bifunctional Pt(II) complexes with a bidentate ligand terminated by pyridyl or imidazolyl rings [with the remaining coordination site(s) occupied by halide(s)] and forming five-, six-, or seven-membered chelate rings^{22–38} have relatively smaller average dihedral angles (Figure 7). However, the three known Pt(II) complexes with eight-membered chelate rings^{42–44} used in the plot have large dihedral angles (73–89°), values close to the dihedral angles observed in the complexes reported here (Figure 7). Furthermore, the dihedral angles of the known bifunctional Pt(II) complexes increase almost linearly with increasing chelate ring size (Figure 7). Therefore, the low degree of tilting in **5** and **6** probably reflects the structural constraints mandated by the relatively large eight-membered chelate ring.

The N1–Pt–N3 bite angle of **5** (87.98°) is at the high end of the range reported for Pt(II) complexes with mono- or bidentate-coordinated ligands terminated by pyridyl or imidazolyl rings (78–91°).^{22–49} The bite angles of known Pt complexes having eight-membered chelate rings (average 89.5°) are higher than for Pt complexes with smaller chelate rings^{22–44} but are quite close to those for monodentate complexes (average 89.4°)^{45–49} (Figure 8). We attribute this finding to the greater spatial freedom provided by the larger

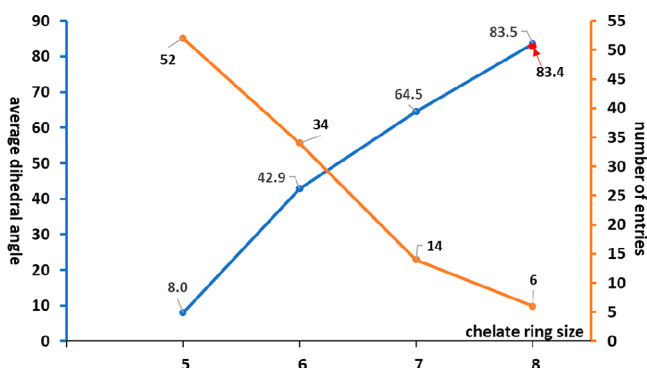


Figure 7. Relationship between average dihedral angle (blue line, left axis, in degrees) and chelate ring size plotted for reported molecular structures of bifunctional Pt(II) complexes with linear bidentate ligands terminated by pyridyl or imidazolyl donor rings (with the remaining two coordination sites occupied by halide ligands). The orange line shows the number of donor rings utilized for each chelate ring size. The red dot shows the average of the dihedral angles for 5 and 6 (83.4°). All of the published data in this figure are from the Cambridge Crystallographic Data Centre, ConQuest 1.19. Of the 108 structures available for complexes with a five-membered chelate ring, data for 26 randomly selected structures were used to prepare the plot.

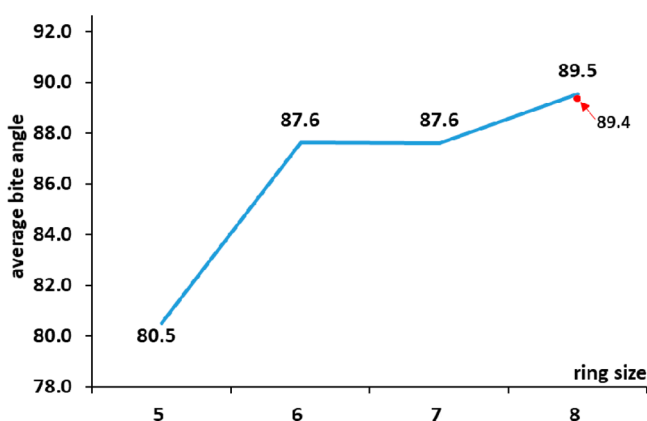


Figure 8. Relationship of the average N–Pt–N bite angle (in degrees, from reported molecular structures) to the chelate ring size of bifunctional Pt(II) complexes of bidentate ligands terminated by pyridyl or imidazolyl donor rings (with the remaining coordination sites occupied by halide ligands). Of the 108 structures available for complexes with a five-membered chelate ring, data for 26 randomly selected structures were used to prepare the plot. The average of the bite angles for eight cis bifunctional Pt(II) complexes of monodentate-bound pyridyl or imidazolyl rings (89.4°) is plotted as a red dot for comparison. All of the published data in this figure are from the Cambridge Crystallographic Data Centre, ConQuest 1.19.

chelate ring; this freedom allows the N-donor rings to be located in the same relative position as monodentate ligands.

Ideally, the Pt–N bond will lie close to the plane of an aromatic N donor ligand to allow the lone pair of the N atom to be positioned for excellent overlap with the Pt(II) bonding orbital, thereby creating a strong bond. The angle between the N-donor aromatic ring plane and the Pt atom is a good structural parameter for assessing how close the Pt is to being in this plane. This angle, defined as the Pt–N–centroid angle (N = N1 or N3, centroid = aromatic ring center) should approach ~180°. The Pt–N–centroid angle ranges from 164–180° for known Pt(II) complexes of imidazolyl or pyridyl

ligands bound in a monodentate, bidentate, or tridentate fashion.^{21–51,62–69} This angle averages 174.5° for **5** (Table 1), which is similar to the value for monodentate ligands (176.7°; see the Supporting Information); this is another indication that the pyridyl rings in **5** are well-positioned to form a strong Pt–N bond.

NMR Spectroscopy. All of the complexes (in DMSO-*d*₆) and ligands (in CDCl₃ and DMSO-*d*₆) reported here were characterized by ¹H NMR spectroscopy. In freshly prepared DMSO-*d*₆ solutions, all of the new complexes gave one set of signals that were consistent with the presence of one time-averaged symmetrical complex and in agreement with the solid-state molecular structure when available. The atom numbering scheme in Figure 2 was used to discuss the NMR data; a modified version of this numbering used for **7a** and **8a** is explained below. Signals were assigned by analyzing chemical shifts, splitting patterns, integrations, and ¹H–¹H NOE cross-peaks. ¹H NMR shifts appear in Table 2 and in the Experimental Section. Key assignment procedures are described in the Supporting Information, along with more NMR data and examples of spectra such as ¹H–¹H ROESY spectra, which are useful for making assignments.

Effects of the Coordination Binding Mode on the Methylene ¹H NMR Signals of Ligands 1–4. Inversion at the sulfonamide N of ligands 1–4 leads to time averaging and makes the methylene protons magnetically equivalent, so the methylene ¹H NMR signal is a singlet. When the ligand is coordinated in a bidentate fashion in the Pt(II) complexes, the methylene protons are no longer made equivalent by a time-averaging process. The protons projecting toward and away from the Cl ligands are designated as *endo*-CH and *exo*-CH protons, respectively (Figure 9). The observation of only one set of ¹H NMR signals (Figure 10 and the Supporting Information) with the *endo*-CH and *exo*-CH protons producing either two doublets (**5**) or an AB pattern (**6**) is consistent with the presence of a symmetrical dichloro complex with a bidentate chelate (Figure 5). Assignments of the AB features/doublets as *endo*-CH or *exo*-CH for **5** and **6** (as explained in the Supporting Information) are presented in Figure 10 and Table 2. The *endo*-CH signal is normally clearly downfield of the *exo*-CH signal for **5**, as previously reported for [Pt(N(H)dpa)]Cl²⁰ and [Pt(N(H)6,6'-Me₂dpa)]Cl^{50,51} complexes. For **6**, these signals, which form an overlapped AB pattern, were assigned by studying the temperature dependence of the chemical shifts (see the Supporting Information).

The ¹H NMR signals of fresh DMSO-*d*₆ solutions of **8** and **8a** (Figure 11) are consistent with single species having the molecular structures of **8** and **8a**, respectively (Figure 6). The NMR data (Table 2) for **7**, **8**, and **8a** (Figure 11) and for **7a** (not shown) establish that the N(SO₂R)6,6'-Me₂dpa ligands coordinate in a monodentate (not bidentate) fashion to form binuclear or mononuclear complexes (Figures 4 and 6). As for the free ligands, the methylene signals for all of the complexes are singlets (Figure 11).

¹H NMR Solution Studies of the Robustness and Reactivity of Pt(II) Complexes of N(SO₂R)3,3',5,5'-Me₄dpa Ligands 1 and 2. ¹H NMR spectra of solutions (10 mM) of Pt(N(SO₂R)3,3',5,5'-Me₄dpa)Cl₂ complexes **5** and **6** indicate that these complexes do not undergo any change over 7 days in DMF-*d*₇ (see the Supporting Information) but do change with time in DMSO-*d*₆. We examined the DMSO-*d*₆ solution chemistry of complex **5** (R = Me) in more detail than **6** because **5** has fewer and simpler

Table 2. Selected ^1H NMR Chemical Shifts (ppm, $\text{DMSO-}d_6$, 25 $^\circ\text{C}$) for $N(\text{SO}_2\text{R})\text{Me}_n\text{dpa}$ Ligands 1–4 and Their Pt(II) Complexes 5–8a

ligand or complex	H6/6'	H5/5'	H4/4'	H3/3'	CH_2	6/6'-Me	SO_2Me
1	8.17	–	7.33	–	4.45	–	3.13
5	8.98	–	7.56	–	5.99, ^a 5.37 ^b	–	3.35
2	7.94	–	7.21	–	4.41	–	–
6	8.90	–	7.56	–	5.55, ^b 5.47 ^a	–	–
3	–	7.12	7.63	7.12	4.42	2.41	3.14
7	–	7.46	7.85	7.68	5.55	3.12	3.33
7a	–	7.49, ^c 7.16 ^d	7.97, ^c 7.60 ^d	7.57, ^c 7.18 ^d	5.44, ^c 4.52 ^d	3.23, ^c 2.44 ^d	3.22
4	–	7.04	7.53	7.04	4.43	2.28	–
8	–	7.43	7.76	7.57	5.46	3.11	–
8a	–	7.42, ^c 7.04 ^d	7.88, ^c 7.54 ^d	7.49, ^c 7.14 ^d	5.40, ^c 4.50 ^d	3.09, ^c 2.27 ^d	–

^aendo-CH. ^bexo-CH. ^cBound. ^dUnbound.

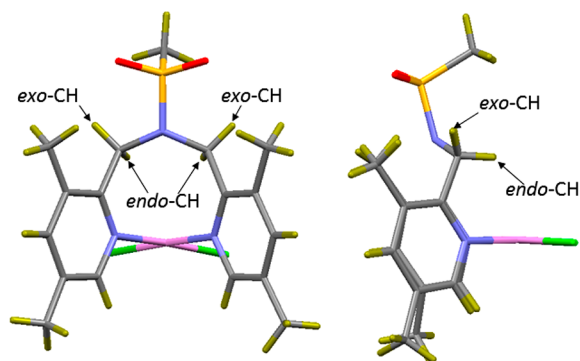


Figure 9. Designation of methylene *endo*-CH and *exo*-CH protons, illustrated using the structure of 5.

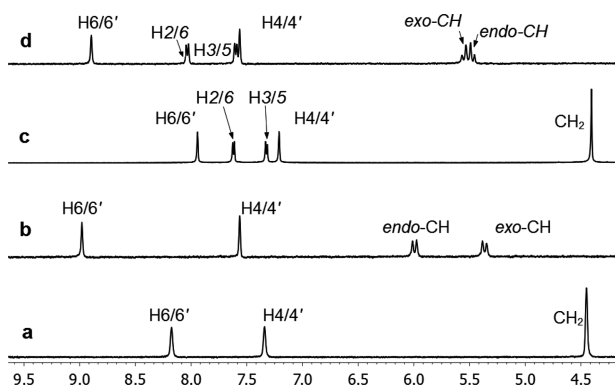


Figure 10. Selected region of the ^1H NMR spectra in $\text{DMSO-}d_6$ at 25 $^\circ\text{C}$ (shifts in ppm) of (a) ligand 1, (b) complex 5, (c) ligand 2, and (d) complex 6.

NMR signals. One hour after “solution 1” (10 mM 5 in $\text{DMSO-}d_6$) was prepared, its spectrum showed, in addition to the peaks for 5, a small but detectable new set of ^1H NMR peaks; these new peaks gradually increased with time (Figure 12). The intensity of the H6/6' singlet of 5 at 8.98 ppm gradually decreased. The shifts at 9.17 and 8.76 ppm of these equally intense growing singlets indicate that the new product contains Pt(II)-bound, geometrically inequivalent pyridyl rings. These new aromatic H6 and H6' signals are consistent with the formation of the solvolysis product $[\text{Pt}(\text{N}(\text{SO}_2\text{Me})\text{-}3,3',5,5'\text{-Me}_4\text{dpa})(\text{DMSO-}d_6)\text{Cl}]^+$ (\mathcal{S}_{sol}). Unlike the H6/6' protons, the H4/4' protons of \mathcal{S}_{sol} give rise to one overlapped signal (7.74 ppm) with an intensity twice that of the H6 or H6' signals. The H4/4' protons are located farther from the Pt(II)

center than are the H6/6' protons, accounting for the presence of an overlapped H4/4' signal. A solution identical to solution 1 was allowed to stand for 24 h, and then 10 molar equiv of $[\text{Et}_4\text{N}]\text{Cl}$ was added (solution 2). The changes at longer times are described briefly below and in more detail in the Supporting Information. Here we note that within 24 h the \mathcal{S}_{sol} ratio changed from $\sim 6:4$ to $\sim 40:1$. The \mathcal{S}_{sol} signals were almost completely absent in another 10 mM solution of 5 (made by dissolving 3.6 mg of solid 5) in a $\text{DMSO-}d_6$ solution containing 100 mM $[\text{Et}_4\text{N}]\text{Cl}$ (solution 3, described in more detail in the Supporting Information). The conversion of \mathcal{S}_{sol} into 5 in solution 2 and the suppression of the formation of \mathcal{S}_{sol} signals in solution 3 together with the features of the \mathcal{S}_{sol} NMR signals all establish without doubt that \mathcal{S}_{sol} is $[\text{Pt}(\text{N}(\text{SO}_2\text{Me})\text{-}3,3',5,5'\text{-Me}_4\text{dpa})(\text{DMSO-}d_6)\text{Cl}]^+$. Pt(II) LCl_2 complexes in which L is an N,N bidentate ligand that have been reported to undergo monosolvolyis in $\text{DMSO-}d_6$ include examples in which the N atoms are in pyridyl rings ($\text{Pt}(\text{bis}(\text{pyridine-}2\text{-yl})\text{amine})\text{Cl}_2$ ³⁷) and in amine groups ($\text{Pt}(\text{ethylenediamine})\text{-Cl}_2$ ⁷⁰ and $\text{Pt}(\text{DNSH-dienH})\text{Cl}_2$ ¹⁰).

The NMR spectral changes over longer times in solutions of 5 in $\text{DMSO-}d_6$ are revealing. In addition to the appearance of NMR signals for \mathcal{S}_{sol} in solution 1 as described above, signals of the free ligand 1 became detectable a few hours after 5 was dissolved (Figure 12). At 24 h, the $\mathcal{S}_{\text{sol}}:1$ ratio was 59:34:7 (Figure 13). At 9 days, the major species was \mathcal{S}_{sol} ($\mathcal{S}_{\text{sol}}:1 = 12:46:42$); this is the equilibrium composition, as no further change in the ratio was detected even after 21 days.

At long times, solution 2 (created by addition of 10 molar equiv of $[\text{Et}_4\text{N}]\text{Cl}$ to a 1-day-old 10 mM solution of 5; see the Supporting Information) exhibited only NMR signals attributable to free 1 at ~ 12 days. In solution 3, in which the formation of \mathcal{S}_{sol} was suppressed, ^1H NMR peaks of free ligand 1 were first detected after a few hours until 100% free 1 was present by ~ 12 days (see the Supporting Information). Collectively, this evidence indicates that the chloride ions facilitate dissociation of ligand 1 from 5 or \mathcal{S}_{sol} .

Two experiments in which 10 mM *cis*-Pt(DMSO) $_2\text{Cl}_2$ and 1 in $\text{DMSO-}d_6$ were followed with time are described in the Supporting Information. Solution 4, also containing 100 mM $[\text{Et}_4\text{N}]\text{Cl}$, showed no NMR signals for 5 or \mathcal{S}_{sol} even after 4 days, indicating that a high chloride ion concentration prevents 1 from coordinating to Pt(II). Results with solution 5, also having *cis*-Pt(DMSO) $_2\text{Cl}_2$ and 1 but no excess of competing chloride ions, indicate that the affinity of ligand 1 at 10 mM for Pt(II) is comparable to that of the $\text{DMSO-}d_6$ molecules in the solvent (“concentration” ~ 14 M).

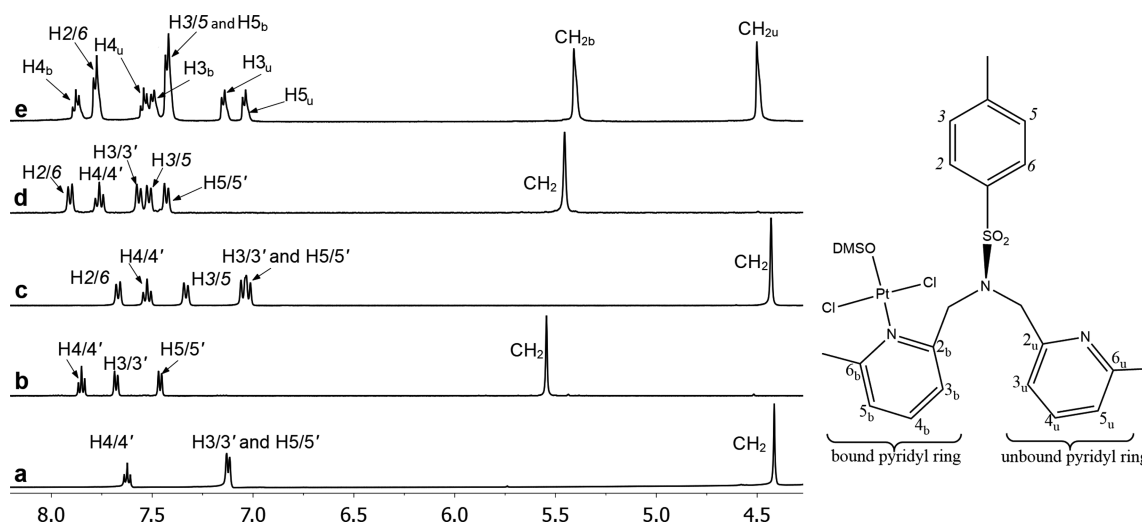


Figure 11. Selected region of the ^1H NMR spectra (ppm, fresh $\text{DMSO}-d_6$ solutions, $25\text{ }^\circ\text{C}$) of (a) ligand 3, (b) complex 7, (c) ligand 4, (d) complex 8, and (e) complex 8a (whose structure is shown as a line drawing at the right).

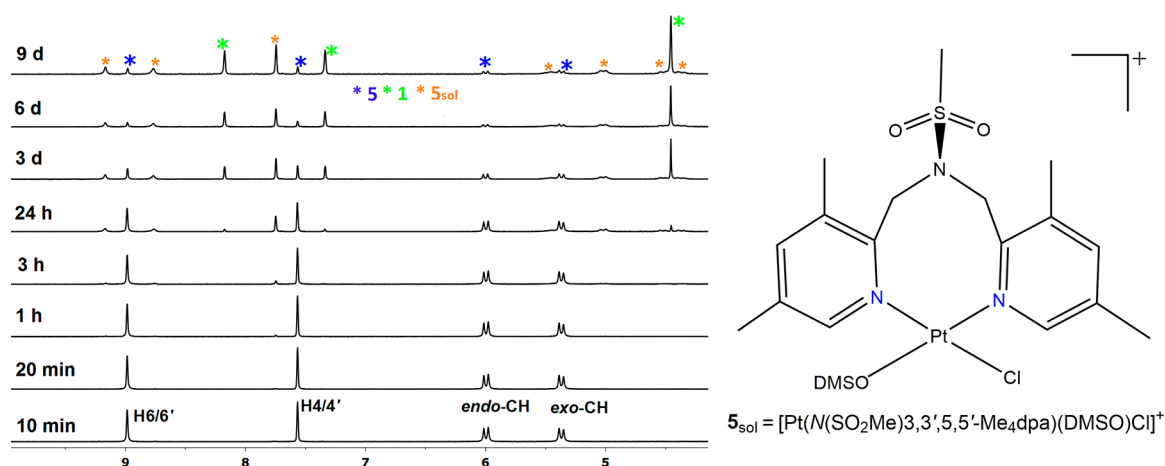


Figure 12. Selected region of the ^1H NMR spectra of solution 1 (10 mM **5** in $\text{DMSO}-d_6$) at $25\text{ }^\circ\text{C}$ (shifts in ppm). Spectra at various times after dissolution of **5** reveal its solvolysis to form $[\text{Pt}(\text{N}(\text{SO}_2\text{Me})_{3,3',5,5'}\text{-Me}_4\text{dpa})(\text{DMSO})\text{Cl}]^+$ (5_{sol}) (shown as a line drawing at the right) and free ligand **1**. The top trace at 9 days corresponds to the equilibrated solution.

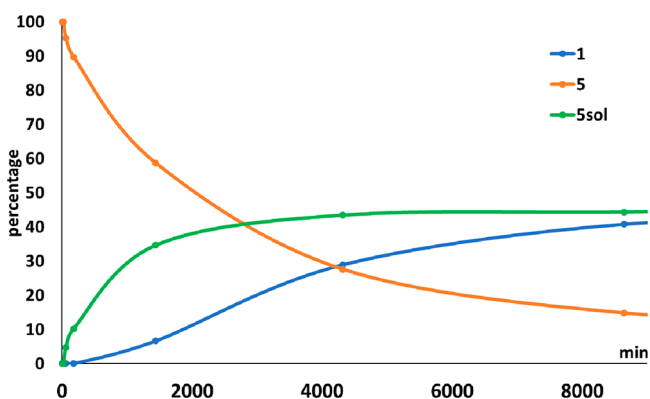


Figure 13. Percent distribution of **5** (orange), 5_{sol} (green), and free ligand **1** (blue) in solution 1 (10 mM **5** in $\text{DMSO}-d_6$) at $25\text{ }^\circ\text{C}$ plotted vs time. Percent distribution values were calculated from integrations of the $\text{H}4/4'$ signals of each species.

The Pt–N–centroid angles of **5** are similar to the values for other bifunctional Pt(II) complexes of monodentate pyridyl ligands, which have five-membered,^{20–22,51} six-membered,^{27,37}

or seven-membered⁴⁹ chelate rings and can adopt optimal metrics not limited by the chelate ring (see the [Supporting Information](#)). These structural metrics as well as the downfield shifts of NMR signals noted above indicate that **5** has enthalpically favorable pyridyl–Pt bonding interactions. As discussed in the [Supporting Information](#), there is evidence that a head-to-head geometry of two cis pyridyl ligands with α -carbon substituents such as the methylene groups of the $-\text{CH}_2-\text{N}(\text{SO}_2\text{R})-\text{CH}_2-$ chain is sterically unfavorable. Thus, the unfavorable entropy component of an eight-membered chelate ring and possibly steric strain within the large chelate ring itself most likely account for the low robustness of **5** and **6** in $\text{DMSO}-d_6$.

The reactivity of **5** with simple G derivatives was assessed at $25\text{ }^\circ\text{C}$ by ^1H NMR spectroscopy. In $\text{DMF}-d_7$, a 1:2.5 mol/mol mixture of **5** (5 mM) and guanosine (Guo) (the solution was cloudy because of poor solubility) was monitored and exhibited no changes even after 4 days. In $\text{DMSO}-d_6$, **5** (10 mM) was treated with 2.5 molar equiv of 9-MeG or Guo. For both solutions, new ^1H NMR peaks for 5_{sol} and free **1** were first detectable after ~ 1 and ~ 4 h, respectively. These results are very similar to those observed in the absence of added 9-

MeG or Guo. Several new peaks consistent with the formation of G adducts were observed only at later times. However, even at 24 h the integration of these new peaks indicated a very low amount of G adduct formation compared with the reactions forming S_{sol} and free ligand 1. Results similar to those just described for reaction mixtures of 5 with G derivatives were found with other ligands known to bind Pt(II) (1-methylimidazole, 5,5'-Me₂bpy, and Me₄dt).^{22,38,71} These results in DMF-*d*₇ and DMSO-*d*₆ indicate that G derivatives and other ligands do not promote chelate ring opening in 5. In contrast, 9-EtG (2.5 equiv) immediately promoted chelate ring opening of the tridentate ligand in [Pt(N(H)6,6'-Me₂dpa)-Cl]Cl.⁵¹

Solution Studies of the Robustness of Pt(II) Complexes of N(SO₂R)6,6'-Me₂dpa Ligands 3 and 4. Whereas complexes 5 and 6 released bidentate-bound ligands 1 and 2 only partially (~40%), the release of monodentate-bound ligands 3 and 4 from 7 and 8, respectively, was essentially complete (>90%). This result indicates that the complexes formed by bidentate ligands 1 and 2 are more thermodynamically stable than the complexes formed by monodentate ligands 3 and 4, as might be expected. The Pt–N bond distances are 0.03 to 0.05 Å longer in 8 and 8a than in 5 and 6 (Table 2). Although the differences are not all statistically significant, there are enough consistent reports on Pt(II) structures to suggest that having a monodentate pyridine substituted at both the 2- and 6-positions with groups having CH₂Y (Y = various groups, the simplest being OH) will increase the Pt–N bond distance by ~0.02 to ~0.03 Å and that having a trans DMSO ligand will add a further ~0.01 to ~0.02 Å.^{72–75} Therefore, it is likely that the known trans influence of the DMSO ligand^{76,77} and the steric effect of the substituents at the 2,6-positions weaken the Pt–N bond and thus lead to the more complete release of ligands 3 and 4 compared with ligands 1 and 2. However, the monodentate ligands 3 and 4 were released from complexes 7 and 8, respectively, less quickly than the bidentate-bound ligands 1 and 2 were released from complexes 5 and 6, respectively. These results and the role that the 6/6' methyl groups play in slowing ligand release and also in favoring monodentate over bidentate binding by ligands 1 and 2 are presented in the Supporting Information.

CONCLUSIONS

Past work has almost always incorporated tertiary sulfonamide linking groups within macrocyclic ligands in order to overcome the weak N(sulfonamide)-donor ability; such complexes have distorted geometries and long M–N(sulfonamide) bonds (even for the tight tacn macrocyclic ring).^{58,60,78} Pt(II) complexes with tetradentate macrocyclic ligands lack functional leaving ligands needed for reactions with biomolecules; such reactivity is a major reason why Pt(II) compounds have enjoyed wide use in both therapeutic and diagnostic applications. In this work, we explored the extension of N(SO₂R)dpa-type tridentate ligand chemistry to Pt(II) chloro compounds by using synthetic conditions applicable to complexes intended for biological applications and known to lead to Pt(II) complexes with chloride leaving ligands. Under these conditions with N(SO₂R)3,3',5,5'-Me₄dpa ligands, a Pt–N(sulfonamide) bond did not form. Instead, the ligands bound in a bidentate fashion, creating Pt(II) chloro complexes with rarely observed eight-membered chelate rings.

From an extensive analysis of structural data of relevant Pt(II) complexes, we conclude that the pyridyl groups in the new complexes occupy locations that allow the formation of favorable Pt–N(pyridyl) bonds. We conclude that steric repulsions within the –CH₂–N(SO₂R)–CH₂– chain of the eight-membered chelate ring may be sufficiently unfavorable to overcome the likely small entropy term favoring the large eight-membered chelate ring. As a consequence, an unusual equilibrium is established between an N,N bidentate chelate ligand bound in a Pt(II) complex and that ligand free in solution.

The chelate ring in complexes 5 and 6 appears to restrict the dihedral angle between the coordination plane and the plane of the pyridyl rings to high values near 90°. Thus, the pyridyl rings could sterically hinder the binding of N-donor ligands to 5 and 6. The N-donor nucleobase of guanosine is relatively large, explaining the observed very unusual, perhaps even unique, lack of reactivity of these Pt(II) chloro complexes toward guanosine. Both the bidentate ligand release and the lack of reactivity toward guanosine thus must be circumvented in future ligand design. Because the ligands form bifunctional (not monofunctional) Pt(II) complexes, we believe that new ligands with smaller terminal donor groups will improve both the stability and reactivity of the complexes while increasing the potential utility of the complexes in biological applications.

A possible contributing reason why the N(SO₂R)dpa-type ligands did not form a Pt(II)–N(sulfonamide) bond is that the N(sulfonamide) group would be a very poor donor if the group were to anchor two adjacent five-membered chelate rings in a meridional geometry. This suggestion is consistent with extensive reported structural information on complexes with a M–N(tertiary sulfonamide) bond; these results suggest to us that the tertiary sulfonamide N-donor enforces facial coordination. Because only a very few types of anchoring donor groups in linear multidentate chelate ligands are known to enforce facial stereochemistry,⁷⁹ further studies assessing tertiary sulfonamide donors within linear chelate ligands are warranted.

ASSOCIATED CONTENT

Supporting Information

The Supporting Information is available free of charge on the ACS Publications website at DOI: 10.1021/acs.inorgchem.8b01943.

Table of selected crystal data and structure refinement parameters for complexes 5, 6, 8, and 8a; plot relating the average Pt–N-centroid angle to the chelate ring size of Pt(II) complexes; selected regions of 1D or 2D ¹H NMR spectra of complexes 5, 6, 7, 8, and 8a; ¹H NMR signal assignments for 5–8a; more complete ¹H NMR shift data for ligands 1–4 and complexes 5–8 (in DMSO-*d*₆ and DMF-*d*₇); description of changes with time in complexes of ligands 1–4 in DMSO-*d*₆, including effects of added [Et₄N]Cl; and discussion of possible reasons favoring monodentate coordination of ligands 3 and 4 to Pt(II) (PDF)

Accession Codes

CCDC 1855002–1855004 and 1855006 contain the supplementary crystallographic data for this paper. These data can be obtained free of charge via www.ccdc.cam.ac.uk/data_request/cif, or by e-mailing data_request@ccdc.cam.ac.uk, or by contacting The Cambridge Crystallographic Data Centre, 12

Union Road, Cambridge CB2 1EZ, U.K.; fax: +44 1223 336033.

AUTHOR INFORMATION

Corresponding Author

*E-mail: lmarzil@lsu.edu.

ORCID

Kokila Ranasinghe: 0000-0001-9021-0076

Patricia A. Marzilli: 0000-0002-8103-9606

Luigi G. Marzilli: 0000-0002-0406-0858

Notes

The authors declare no competing financial interest.

ACKNOWLEDGMENTS

Upgrade of the diffractometer was made possible through Grant LEQSF(2011-12)-ENH-TR-01, administered by the Louisiana Board of Regents. We thank Dr. Frank Fronczek for his help with some aspects of the X-ray structural studies.

REFERENCES

- (1) Veltze, S.; Egdal, R. K.; Johansson, F. B.; Bond, A. D.; McKenzie, C. J. Coordinative Flexibility in an Acyclic Bis(sulfonamide) Ligand. *Dalton Trans.* **2009**, 10495–10504.
- (2) Lu, G.; Hillier, S. M.; Maresca, K. P.; Zimmerman, C. N.; Eckelman, W. C.; Joyal, J. L.; Babich, J. W. Synthesis and SAR of Novel Re^{99m}Tc-Labeled Benzenesulfonamide Carbonic Anhydrase IX Inhibitors for Molecular Imaging of Tumor Hypoxia. *J. Med. Chem.* **2013**, *56*, 510–520.
- (3) Langdon-Jones, E. E.; Symonds, N. O.; Yates, S. E.; Hayes, A. J.; Lloyd, D.; Williams, R.; Coles, S. J.; Horton, P. N.; Pope, S. J. A. Fluorescent Rhenium–Naphthalimide Conjugates as Cellular Imaging Agents. *Inorg. Chem.* **2014**, *53*, 3788–3797.
- (4) Perera, T.; Abhayawardhana, P.; Marzilli, P. A.; Fronczek, F. R.; Marzilli, L. G. Formation of a Metal-to-Nitrogen Bond of Normal Length by a Neutral Sulfonamide Group within a Tridentate Ligand. A New Approach to Radiopharmaceutical Bioconjugation. *Inorg. Chem.* **2013**, *52*, 2412–2421.
- (5) Abhayawardhana, P. L.; Marzilli, P. A.; Fronczek, F. R.; Marzilli, L. G. Complexes Possessing Rare “Tertiary” Sulfonamide Nitrogen-to-Metal Bonds of Normal Length: *fac*-[Re(CO)₃(N(SO₂R)₂dien)]PF₆ Complexes with Hydrophilic Sulfonamide Ligands. *Inorg. Chem.* **2014**, *53*, 1144–1155.
- (6) Bartholoma, M.; Valliant, J.; Maresca, K. P.; Babich, J.; Zubieta, J. Single Amino Acid Chelates (SAAC): A Strategy for the Design of Technetium and Rhenium Radiopharmaceuticals. *Chem. Commun.* **2009**, *5*, 493–512.
- (7) Maresca, K. P.; Marquis, J. C.; Hillier, S. M.; Lu, G.; Femia, F. J.; Zimmerman, C. N.; Eckelman, W. C.; Joyal, J. L.; Babich, J. W. Novel Polar Single Amino Acid Chelates for Technetium-99m Tricarbonyl-Based Radiopharmaceuticals with Enhanced Renal Clearance: Application to Octreotide. *Bioconjugate Chem.* **2010**, *21*, 1032–1042.
- (8) Maresca, K. P.; Kronauge, J. F.; Zubieta, J.; Babich, J. W. Novel Ether-Containing Ligands as Potential ^{99m}Technetium(I) Heart Agents. *Inorg. Chem. Commun.* **2007**, *10*, 1409–1412.
- (9) Zhu, J.; Zhao, Y.; Zhu, Y.; Wu, Z.; Lin, M.; He, W.; Wang, Y.; Chen, G.; Dong, L.; Zhang, J.; Lu, Y.; Guo, Z. DNA Cross-Linking Patterns Induced by an Antitumor-Active Trinuclear Platinum Complex and Comparison with Its Dinuclear Analogue. *Chem. - Eur. J.* **2009**, *15*, 5245–5253.
- (10) Christoforou, A. M.; Marzilli, P. A.; Marzilli, L. G. The Neglected Pt–N(sulfonamido) Bond in Pt Chemistry. New Fluorophore-Containing Pt(II) Complexes Useful for Assessing Pt(II) Interactions with Biomolecules. *Inorg. Chem.* **2006**, *45*, 6771–6781.
- (11) Olivova, R.; Kasparkova, J.; Vrana, O.; Vojtiskova, M.; Suchankova, T.; Novakova, O.; He, W.; Guo, Z.; Brabec, V. Unique DNA Binding Mode of Antitumor Trinuclear Tridentate Platinum(II) Compound. *Mol. Pharmaceutics* **2011**, *8*, 2368–2378.
- (12) Zhao, Y.; He, W.; Shi, P.; Zhu, J.; Qiu, L.; Lin, L.; Guo, Z. A Positively Charged Trinuclear 3N-Chelated Monofunctional Platinum Complex with High DNA Affinity and Potent Cytotoxicity. *Dalton Trans.* **2006**, 2617–2619.
- (13) Wu, S.; Zhu, C.; Zhang, C.; Yu, Z.; He, W.; He, Y.; Li, Y.; Wang, J.; Guo, Z. In Vitro and in Vivo Fluorescent Imaging of a Monofunctional Chelated Platinum Complex Excitable Using Visible Light. *Inorg. Chem.* **2011**, *50*, 11847–11849.
- (14) Ndinguri, M. W.; Fronczek, F. R.; Marzilli, P. A.; Crowe, W. E.; Hammer, R. P.; Marzilli, L. G. Exploring Water-Soluble Pt(II) Complexes of Diethylenetriamine Derivatives Functionalized at the Central Nitrogen. Synthesis, Characterization, and Reaction with 5'-GMP. *Inorg. Chim. Acta* **2010**, *363*, 1796–1804.
- (15) van der Schilden, K.; Garcia, F.; Kooijman, H.; Spek, A. L.; Haasnoot, J. G.; Reedijk, J. A Highly Flexible Dinuclear Ruthenium(II)–Platinum(II) Complex: Crystal Structure and Binding to 9-Ethylguanine. *Angew. Chem., Int. Ed.* **2004**, *43*, 5668–5670.
- (16) Reddy G, U.; Axthelm, J.; Hoffmann, P.; Taye, N.; Gläser, S.; Görls, H.; Hopkins, S. L.; Plass, W.; Neugebauer, U.; Bonnet, S.; Schiller, A. Co-Registered Molecular Logic Gate with a CO-Releasing Molecule Triggered by Light and Peroxide. *J. Am. Chem. Soc.* **2017**, *139*, 4991–4994.
- (17) Reddy G, U.; Liu, J.; Hoffmann, P.; Steinmetzer, J.; Gorls, H.; Kupfer, S.; Askes, S. H. C.; Neugebauer, U.; Grafe, S.; Schiller, A. Light-Responsive Paper Strips as CO-Releasing Material with a Colourimetric Response. *Chem. Sci.* **2017**, *8*, 6555–6560.
- (18) Reedijk, J. Increased Understanding of Platinum Anticancer Chemistry. *Pure Appl. Chem.* **2011**, *83*, 1709–1719.
- (19) Damian, M. S.; Hedman, H. K.; Elmroth, S. K. C.; Diederichsen, U. Synthesis and DNA Interaction of Platinum Complex/Peptide Chimera as Potential Drug Candidates. *Eur. J. Org. Chem.* **2010**, *2010*, 6161–6170.
- (20) Andrepont, C.; Marzilli, P. A.; Marzilli, L. G. Guanine Nucleobase Adducts Formed by [Pt(di-(2-picolyl)amine)Cl]Cl: Evidence That a Tridentate Ligand with Only in-Plane Bulk Can Slow Guanine Base Rotation. *Inorg. Chem.* **2012**, *51*, 11961–11970.
- (21) Ranasinghe, K.; Marzilli, P. A.; Pakhomova, S.; Marzilli, L. G. A Very Rare Example of a Structurally Characterized 3'-GMP Metal Complex. NMR and Synthetic Assessment of Adducts Formed by Guanine Derivatives with [Pt(L^{tri})Cl]Cl complexes with L^{tri} = N,N',N'' Tridentate Ligand Terminated by Imidazole Rings. *Inorg. Chem.* **2017**, *56*, 8462–8477.
- (22) Bhattacharyya, D.; Marzilli, P. A.; Marzilli, L. G. Exploring the Universality of Unusual Conformations of the 17-Membered Pt(d(G*_pG*)) Macrochelate Ring. Dependence of Conformer Formation on a Change in Bidentate Carrier Ligand from an sp³ to an sp² Nitrogen Donor. *Inorg. Chem.* **2005**, *44*, 7644–7651.
- (23) Tu, C.; Wu, X.; Liu, Q.; Wang, X.; Xu, Q.; Guo, Z. Crystal Structure, DNA-Binding Ability and Cytotoxic Activity of Platinum(II) 2,2'-Dipyridylamine Complexes. *Inorg. Chim. Acta* **2004**, *357*, 95–102.
- (24) Rauterkus, M. J.; Fakhri, S.; Mock, C.; Puscasu, I.; Krebs, B. Cisplatin Analogues with 2,2'-Dipyridylamine Ligands and Their Reactions with DNA Model Nucleobases. *Inorg. Chim. Acta* **2003**, *350*, 355–365.
- (25) Kelly, M. E.; Gómez-Ruiz, S.; Steinborn, D.; Wagner, C.; Schmidt, H. Synthesis, Characterization and X-ray Crystal Structures of Polyether and Ethylene Bridged Bis(azolyl) Platinum(II) Complexes. *Transition Met. Chem.* **2008**, *33*, 721–727.
- (26) Bulak, E.; Leboschka, M.; Schwederski, B.; Sarper, O.; Varnali, T.; Fiedler, J.; Lissner, F.; Schleid, T.; Kaim, W. Reversibly Reducible cis-Dichloroplatinum(II) and cis-Dichloropalladium(II) Complexes of Bis(1-methylimidazol-2-yl)glyoxal. *Inorg. Chem.* **2007**, *46*, 5562–5566.
- (27) Bloemink, M. J.; Engelsing, H.; Karentzopoulos, S.; Krebs, B.; Reedijk, J. Synthesis, Crystal Structure, Antitumor Activity, and DNA-Binding Properties of the New Active Platinum Compound(Bis(N-

methylimidazol-2-yl)carbinol)dichloroplatinum(II), Lacking a NH Moiety, and of the Inactive Analog Dichloro($N^i, N^{i'}$ -dimethyl-2,2'-biimidazole)platinum(II). *Inorg. Chem.* **1996**, *35*, 619–627.

(28) Maheshwari, V.; Bhattacharyya, D.; Fronczek, F. R.; Marzilli, P. A.; Marzilli, L. G. Chemistry of HIV-1 Virucidal Pt Complexes Having Neglected Bidentate sp^2 N-Donor Carrier Ligands with Linked Triazine and Pyridine Rings. Synthesis, NMR Spectral Features, Structure, and Reaction with Guanosine. *Inorg. Chem.* **2006**, *45*, 7182–7190.

(29) McFarlane, A.; Lusty, J. R.; Fiol, J. J.; Terrón, A.; Molins, E.; Miravittles, C.; Moreno, V. Pd(II) and Pt(II) Complexes of 1,2-Bis(pyridin-2-yl)ethane- N, N' . *Z. Naturforsch., B: J. Chem. Sci.* **1994**, *49*, 844–848.

(30) Safa, M.; Jennings, M. C.; Puddephatt, R. J. Reactivity of a Dimethylplatinum(II) Complex with the Bis(2-pyridyl)dimethylsilane Ligand: Easy Silicon–Carbon Bond Activation. *Organometallics* **2012**, *31*, 3539–3550.

(31) Tabatabaei Rezaei, S. J.; Amani, V.; Nabid, M. R.; Safari, N.; Niknejad, H. Folate-Decorated Polymeric Pt(II) Prodrug Micelles for Targeted Intracellular Delivery and Cytosolic Glutathione-Triggered Release of Platinum Anticancer Drugs. *Polym. Chem.* **2015**, *6*, 2844–2853.

(32) Grzesiak, A. L.; Matzger, A. J. Selection and Discovery of Polymorphs of Platinum Complexes Facilitated by Polymer-Induced Heteronucleation. *Inorg. Chem.* **2007**, *46*, 453–457.

(33) Canty, A. J.; Gardiner, M. G.; Jones, R. C.; Sharma, M. Structural Chemistry of $[MX_2(\text{bipy})]$ ($M = \text{Pd, Pt}$; $X = \text{Cl, Br, I}$): the Yellow Polymorph of Dichlorido(2,2'-bipyridine)platinum(II) and Diiodido(2,2'-bipyridine)palladium(II), and Overview of this System. *Aust. J. Chem.* **2011**, *64*, 1355–1359.

(34) Andrade-López, N.; Alvarado-Rodríguez, J. G.; González-Montiel, S.; Páez-Hernández, E.; Galán-Vidal, C. A.; Jiménez-Pérez, A. Synthesis and Crystal Structures of *cis*-Palladium(II) and *cis*-Platinum(II) Complexes Containing Dipyridyl Ligands. *ARKIVOC* **2008**, *2008* (v), 43–54.

(35) Bulak, E.; Varnali, T.; Schwederski, B.; Sarkar, B.; Hartenbach, I.; Fiedler, J.; Kaim, W. 2,3-Bis(1-methylimidazol-2-yl)quinoxaline (bmiq), a New Ligand with Decoupled Electron Transfer and Metal Coordination Sites: the Very Different Redox Behaviour of Isoelectronic Complexes with $[\text{PtCl}_2]$ and $[\text{AuCl}_2]^+$. *Dalton Trans.* **2011**, *40*, 2757–2763.

(36) Casas, J. S.; Castineiras, A.; Parajo, Y.; Sordo, J.; Varela, J. M. (1,1'-Dimethyl-2,2'-biimidazole- N_3, N_3')diiodoplatinum(II). *Acta Crystallogr., Sect. C: Cryst. Struct. Commun.* **1998**, *54*, 1777–1779.

(37) Roy, S.; Westmaas, J. A.; Buda, F.; Reedijk, J. Platinum(II) compounds with chelating ligands based on pyridine and pyrimidine: Synthesis, characterizations, DFT calculations, cytotoxic assays and binding to a DNA model base. *J. Inorg. Biochem.* **2009**, *103*, 1278–1287.

(38) Maheshwari, V.; Marzilli, P. A.; Marzilli, L. G. Neglected Bidentate sp^2 N-Donor Carrier Ligands with Triazine Nitrogen Lone Pairs: Platinum Complexes Retromodeling Cisplatin Guanine Nucleobase Adducts. *Inorg. Chem.* **2008**, *47*, 9303–9313.

(39) Song, D.; Wang, S. Benzene C–H Activation by Two Isomeric Platinum(II) Complexes of Bis(N -7-azaindolyl)methane. *Organometallics* **2003**, *22*, 2187–2189.

(40) Zhao, S.-B.; Liu, G.-h.; Song, D.; Wang, S. Impact of the Linker Groups in Bis(7-azaindol-1-yl) Chelate Ligands on Structures and Stability of $\text{Pt}(N, N-L)_2$ Complexes. *Dalton Trans.* **2008**, 6953–6965.

(41) Davies, M. S.; Fenton, R. R.; Huq, F.; Ling, E. C. H.; Hambley, T. W. Studies on the Nature and Strength of Pt...H(N) Interactions. The Crystal Structures of Chloro[N -(2-aminoethyl)- N -(2-ammonioethyl)ethane-1,2-diamine]platinum(II) Chloride and Dichloro[4,7-diaza-1-azoniacyclononane]platinum(II) Tetrachlor. *Aust. J. Chem.* **2000**, *53*, 451–456.

(42) Moriguchi, T.; Kitamura, S.; Sakata, K.; Tsuge, A. Syntheses and Structures of Dichloropalladium(II)(dithia[3.3]-

metadipyridinophane) and Dichloroplatinum(II)(dithia[3.3]-metadipyridinophane) Complexes. *Polyhedron* **2001**, *20*, 2315–2320.

(43) Zhao, S.-B.; Wang, R.-Y.; Wang, S. Reactivity of SiMe_3 - and SnR_3 -Functionalized Bis(7-azaindol-1-yl)methane with $[\text{PtR}_2(\mu\text{-SMe}_2)]_n$ ($R = \text{Me, Ph}$) and the Resulting Pt(II) and Pt(IV) Complexes. *Organometallics* **2009**, *28*, 2572–2582.

(44) Yang, Y.; Lu, C.; Wang, H.; Liu, X. Amide Bond Cleavage Initiated by Coordination with Transition Metal Ions and Tuned by an Auxiliary Ligand. *Dalton Trans.* **2016**, *45*, 10289–10296.

(45) Sakai, K.; Yokoyama, Y.; Masaoka, S. *cis*-Dichlorobis(4-methylpyridine- κN)platinum(II). *Acta Crystallogr., Sect. E: Struct. Rep. Online* **2007**, *63*, m97–m99.

(46) Tessier, C.; Rochon, F. D. Multinuclear NMR Study and Crystal Structures of Complexes of the Types *cis*- and *trans*- $\text{Pt}(\text{Ypy})_2\text{X}_2$, Where Ypy = Pyridine Derivative and $X = \text{Cl}$ and I . *Inorg. Chim. Acta* **1999**, *295*, 25–38.

(47) Colamarino, P.; Orioli, P. L. Crystal and Molecular Structures of *cis*- and *trans*-Dichlorobispyridine-Platinum(II). *J. Chem. Soc., Dalton Trans.* **1975**, 1656–1659.

(48) Graves, B. J.; Hodgson, D. J.; Van Kralingen, C. G.; Reedijk, J. Synthesis and Structural Characterization of *cis*-dichlorobis(N -methylimidazole)platinum(II) and *cis*-dibromobis(N -methylimidazole)platinum(II). *Inorg. Chem.* **1978**, *17*, 3007–3011.

(49) Marcellis, A. T. M.; Van Der Veer, J. L.; Zwetsloot, J. C. M.; Reedijk, J. Rotation and Conformation of Puke Ligands in *cis*-Bis(6-oxopurine)-Platinum Compounds. *Inorg. Chim. Acta* **1983**, *78*, 195–203.

(50) Andrepont, C.; Marzilli, P. A.; Pakhomova, S.; Marzilli, L. G. Guanine Nucleobase Adducts Formed by a Monofunctional Complex: $[\text{Pt}(N-(6\text{-methyl-2-picolyl})-N-(2\text{-picolyl})\text{amine})\text{Cl}]\text{Cl}$. *J. Inorg. Biochem.* **2015**, *153*, 219–230.

(51) Andrepont, C.; Pakhomova, S.; Marzilli, P. A.; Marzilli, L. G. Unusual Example of Chelate Ring Opening upon Coordination of the 9-Ethylguanine Nucleobase to $[\text{Pt}(\text{di}(6\text{-methyl-2-picolyl})\text{amine})\text{Cl}]\text{Cl}$. *Inorg. Chem.* **2015**, *54*, 4895–4908.

(52) Price, J. H.; Williamson, A. N.; Schramm, R. F.; Wayland, B. B. Palladium(II) and Platinum(II) Alkyl Sulfoxide Complexes. of Sulfur-Bonded, Mixed Sulfur- and Oxygen-Bonded, and Totally Oxygen-Bonded Complexes. *Inorg. Chem.* **1972**, *11*, 1280–1284.

(53) Komatsu, K.; Kikuchi, K.; Kojima, H.; Urano, Y.; Nagano, T. Selective Zinc Sensor Molecules with Various Affinities for Zn^{2+} , Revealing Dynamics and Regional Distribution of Synaptically Released Zn^{2+} in Hippocampal Slices. *J. Am. Chem. Soc.* **2005**, *127*, 10197–10204.

(54) Stock, N. S.; Bain, G.; Zunic, J.; Li, Y.; Ziff, J.; Roppe, J.; Santini, A.; Darlington, J.; Prodanovich, P.; King, C. D.; Baccei, C.; Lee, C.; Rong, H.; Chapman, C.; Broadhead, A.; Lorrain, D.; Correa, L.; Hutchinson, J. H.; Evans, J. F.; Prasit, P. 5-Lipoxygenase-Activating Protein (FLAP) Inhibitors. Part 4: Development of 3-[3-*tert*-Butylsulfanyl-1-[4-(6-ethoxy-pyridin-3-yl)benzyl]-5-(5-methylpyridin-2-ylmethoxy)-1*H*-indol-2-yl]-2,2-dimethylpropionic Acid (AM803), a Potent, Oral, Once Daily FLAP Inhibitor. *J. Med. Chem.* **2011**, *54*, 8013–8029.

(55) Sheldrick, G. A. A Short History of SHELX. *Acta Crystallogr., Sect. A: Found. Crystallogr.* **2008**, *64*, 112–122.

(56) Lewis, N. A.; Pakhomova, S.; Marzilli, P. A.; Marzilli, L. G. Synthesis and Characterization of Pt(II) Complexes with Pyridyl Ligands: Elongated Octahedral Ion Pairs and Other Factors Influencing ^1H NMR Spectra. *Inorg. Chem.* **2017**, *56*, 9781–9793.

(57) Lee, W.-Z.; Tseng, H.-S.; Kuo, T.-S. Ligand-Controlled Nuclearity in Nickel Bis(benzimidazolyl) Complexes. *Dalton Trans.* **2007**, 2563–2570.

(58) Seidler-Egdal, R. K.; Johansson, F. B.; Veltze, S.; Skou, E. M.; Bond, A. D.; McKenzie, C. J. Tunability of the $\text{M}^{\text{II}}\text{M}^{\text{III}}/\text{M}^{\text{I}}_2$ and $\text{M}^{\text{III}}_2/\text{M}^{\text{II}}\text{M}^{\text{III}}$ ($M = \text{Mn, Co}$) Couples in Bis- μ - O, O' -carboxylato- μ -OR Bridged Complexes. *Dalton Trans.* **2011**, *40*, 3336–3345.

(59) Canovese, L.; Visentin, F.; Chessa, G.; Uguagliati, P.; Levi, C.; Dolmella, A.; Bandoli, G. Role of the Ligand and of the Size and Flexibility of the Palladium-Ancillary Ligand Cycle on the Reactivity

of Substituted Alkynes toward Palladium(0) Complexes Bearing Potentially Terdentate Nitrogen-Sulfur-Nitrogen or Nitrogen-Nitrogen-Nitrogen Ligands: Kinetic and Structural Study. *Organometallics* **2006**, *25*, 5355–5365.

(60) Calligaris, M.; Carugo, O.; Crippa, G.; De Santis, G.; Di Casa, M.; Fabbrizzi, L.; Poggi, A.; Seghi, B. 1-(4-Tolylsulfonyl)-1,4,8,11-tetraazacyclotetradecane(Tscyclam): A Versatile Ligand for Nickel(II) and Nickel(III) Cations. *Inorg. Chem.* **1990**, *29*, 2964–2970.

(61) Kim, S.; Minier, M. A.; Loas, A.; Becker, S.; Wang, F.; Lippard, S. J. Achieving Reversible Sensing of Nitroxyl by Tuning the Ligand Environment of Azamacrocyclic Copper(II) Complexes. *J. Am. Chem. Soc.* **2016**, *138*, 1804–1807.

(62) Seubert, K.; Böhme, D.; Kösters, J.; Shen, W.-Z.; Freisinger, E.; Müller, J. N-Methyl-2,2'-Dipicolylamine Complexes as Potential Models for Metal-Mediated Base Pairs. *Z. Anorg. Allg. Chem.* **2012**, *638*, 1761–1767.

(63) Lonnon, D. G.; Craig, D. C.; Colbran, S. B. Rhodium, Palladium and Platinum Complexes of Tris(pyridylalkyl)amine and Tris(benzimidazolylmethyl)amine N₄-Tripodal Ligands. *J. Chem. Soc., Dalton Trans.* **2006**, 3785–3797.

(64) Lo, W. K. C.; Huff, G. S.; Preston, D.; McMorran, D. A.; Giles, G. I.; Gordon, K. C.; Crowley, J. D. A Dinuclear Platinum(II) N₄Py Complex: An Unexpected Coordination Mode For N₄Py. *Inorg. Chem.* **2015**, *54*, 6671–6673.

(65) Yuan, Z.; Shen, X.; Huang, J. Syntheses, Crystal Structures and Antimicrobial Activities of Cu(II), Ru(II), and Pt(II) Compounds with an Anthracene-Containing Tripodal Ligand. *RSC Adv.* **2015**, *5*, 10521–10528.

(66) Zhang, R.; Liang, Z.; Han, A.; Wu, H.; Du, P.; Lai, W.; Cao, R. Structural, Spectroscopic and Theoretical Studies of a Vapochromic Platinum(II) Terpyridyl Complex. *CrystEngComm* **2014**, *16*, 5531–5542.

(67) Petrović, B.; Bugarčić, Ž. D.; Dees, A.; Ivanović-Burmazović, I.; Heinemann, F. W.; Puchta, R.; Steinmann, S. N.; Corminboeuf, C.; van Eldik, R. Role of π -Acceptor Effects in Controlling the Lability of Novel Monofunctional Pt(II) and Pd(II) Complexes: Crystal Structure of [Pt(triipyridinedimethane)Cl]Cl. *Inorg. Chem.* **2012**, *51*, 1516–1529.

(68) Ha, K. Crystal structure of (bis(2-pyridyl)imido)-chloroplatinum(II), PtCl(C₁₂H₈N₃O₂). *Z. Kristallogr. - New Cryst. Struct.* **2011**, *226*, 55–56.

(69) Imler, G. H.; Lu, Z.; Kistler, K. A.; Carroll, P. J.; Wayland, B. B.; Zdilla, M. J. Complexes of 2,5-Bis(α -pyridyl)pyrrolate with Pd(II) and Pt(II): A Monoanionic Iso- π -Electron Ligand Analog of Terpyridine. *Inorg. Chem.* **2012**, *51*, 10122–10128.

(70) Kerrison, S. J. S.; Sadler, P. J. ¹⁹⁵Pt NMR studies of platinum(II) dimethylsulphoxide complexes. *Inorg. Chim. Acta* **1985**, *104*, 197–201.

(71) van Kralingen, G.; Reedijk, J. Coordination compounds of Pt(II) with N-methyl imidazole as a ligand. *Inorg. Chim. Acta* **1978**, *30*, 171–177.

(72) Klein, A.; Elmas, S.; Butsch, K. Oxido Pincer Ligands – Exploring the Coordination Chemistry of Bis(hydroxymethyl)-pyridine Ligands for the Late Transition Metals. *Eur. J. Inorg. Chem.* **2009**, *2009*, 2271–2281.

(73) Grabner, S.; Bukovec, P. The Crystal Structure of a Novel Pt(II) Complex with 2-hydroxy-6-methylpyridine(Hmhp), *trans*-[PtCl₂(dmsO)(Hmhp)]·H₂O. *Acta Chim. Slov.* **2015**, *62*, 389–393.

(74) Rochon, F. D.; Fakhfakh, M. Synthesis and NMR Characterization of the Novel Mixed-Ligand Pt(II) Complexes *cis*- and *trans*-Pt(Ypy)(pyrimidine)Cl₂ and *trans,trans*-Cl₂(Ypy)Pt(μ -pyrimidine)Pt(Ypy)Cl₂ (Ypy = pyridine derivative). *Inorg. Chim. Acta* **2009**, *362*, 1455–1466.

(75) Bostrom, D.; Strandberg, R.; Noren, B.; Oskarsson, A. *Cis/trans* Influences on Square-Planar Platinum(II) Complexes. Structure of *cis*-Bis(dimethyl sulfoxide)dinitratoplatinum(II). *Acta Crystallogr., Sect. C: Cryst. Struct. Commun.* **1991**, *47*, 2101–2104.

(76) Kukushkin, Y. N. Mutual Influence of Ligands in Complexes. *Russ. Chem. Rev.* **1974**, *43*, 805–820.

(77) Manojlovic-Muir, L. J.; Muir, K. W. The *Trans*-Influence of Ligands in Platinum(II) Complexes. The Significance of the Bond Length Data. *Inorg. Chim. Acta* **1974**, *10*, 47–49.

(78) Call, A.; Codolà, Z.; Acuña-Parés, F.; Lloret-Fillol, J. Photo- and Electrocatalytic H₂ Production by New First-Row Transition-Metal Complexes Based on an Aminopyridine Pentadentate Ligand. *Chem. - Eur. J.* **2014**, *20*, 6171–6183.

(79) Toscano, P. J.; Marzilli, L. G. Cobalt(III) Complexes of Stereospecific Linear NSNN Tetradentate Ligands. 1. Synthesis of Ligands That Adopt the *Cis- β* Coordination Geometry. *Inorg. Chem.* **1983**, *22*, 3342–3350.